UNIVERSITY OF MICHIGAN

MichiganEngineering

NERS/BIOE 481

Lecture 11 B
Computed Tomography (CT)

Michael Flynn, Adjunct Prof
Nuclear Engr & Rad. Science
mikef@umich.edu
mikef@rad.hfh.edu

Henry Ford Health System
RADIOLOGY RESEARCH

A) X-ray Computed Tomography ...(L11)

B) CT Reconstruction Methods ...(L11/L12)

B) CT Reconstruction (L12)

1) Projection geometry (5 slides)
2) Fourier Domain Solution
3) Convolution / Backprojection
4) Cone beam reconstruction
5) Iterative Reconstruction

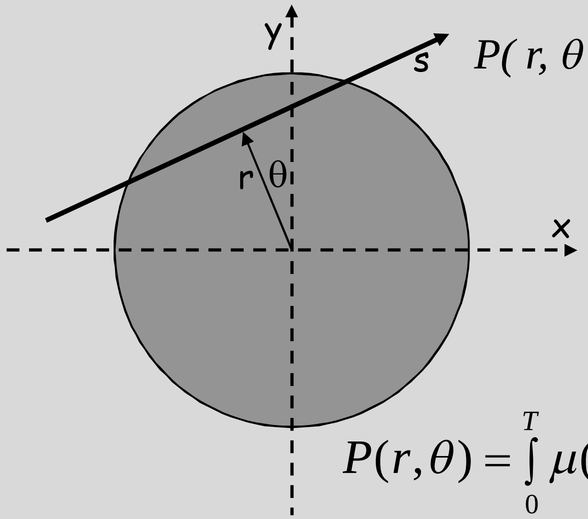

$$P(r,\theta) = \int_0^T \mu(t)dt$$

For an object with a variable attenuation coefficient $\mu(x,y)$, the transmitted x-ray intensity is given by the projection;

$$I(r,\theta) = I_o \ exp[- P(r,\theta)]$$

Thus the projection can be deduced by measuring the transmission;

$$P(r,\theta) = -Log_{nat}[I(r,\theta) / I_o]$$

- CT scanner devices are periodically calibrated using a phantom to determine the reference signal Io.
- The projection, $P(r, \theta)$, is determined using correction factors for x-ray spectral hardening and scattered radiation.

VII.B.1 – Fan beam projection views – 0 & 180 degrees

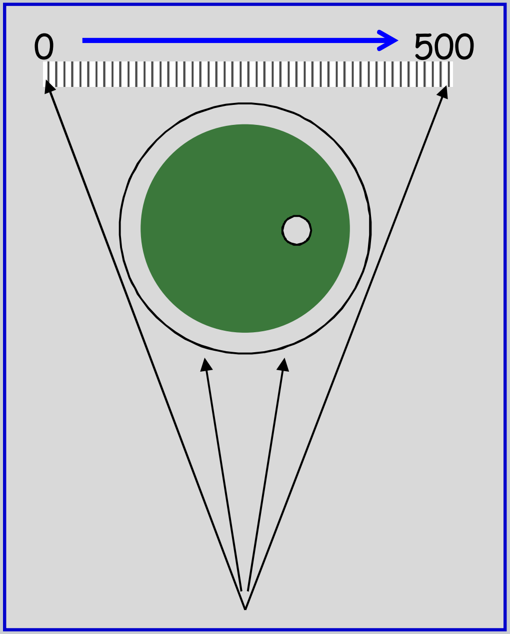

As a CT gantry rotates, the projection of a small target is recorded on the detector at positions that shift from one side to the other.

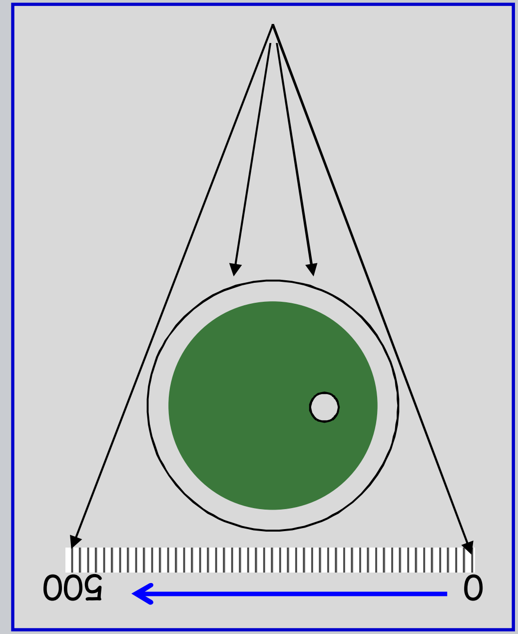

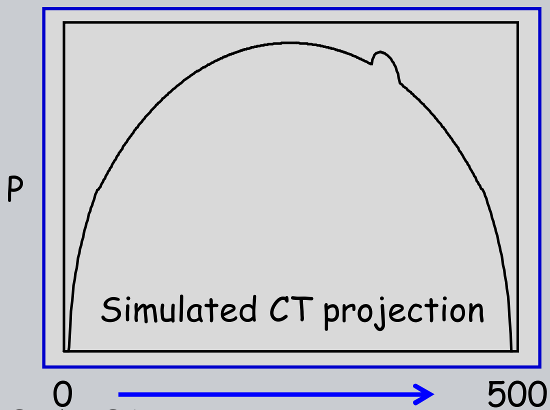

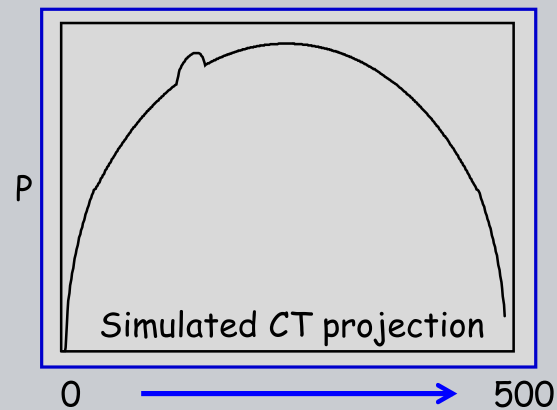

VII.B.1 – Projection views: 0° to 360°

Sinogram:

- An image with the projection values organized as rotation angle versus detector position is referred to as the sinogram.
- The sinogram depicts all of the transmission data used to perform a reconstruction of the object attenuation values.

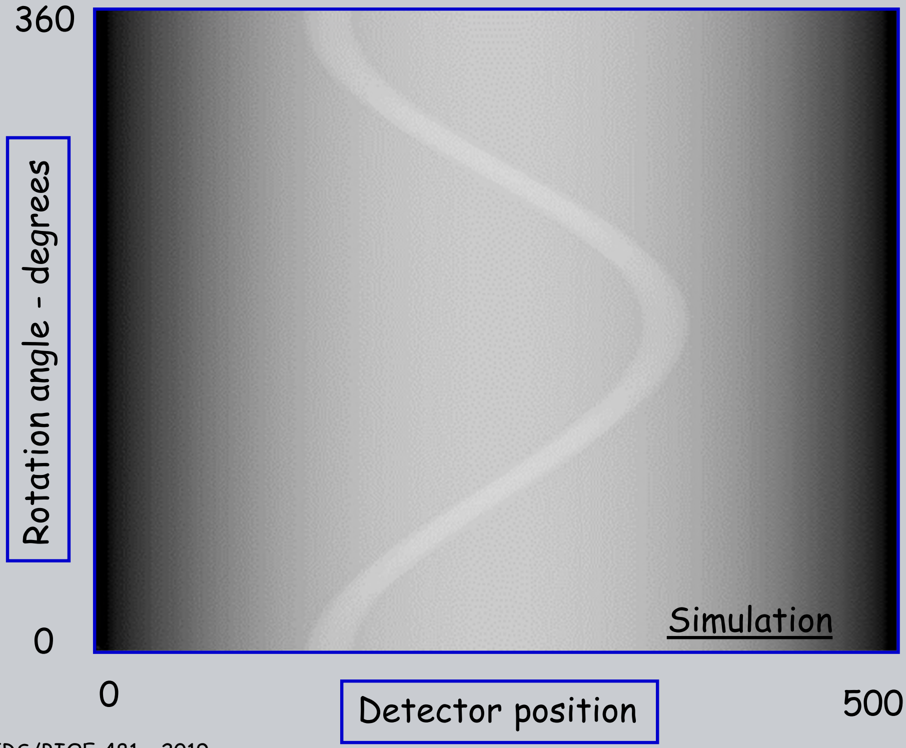

sinogram of a more complex object

VII.B.1 – Inverse solution (computed tomogram)

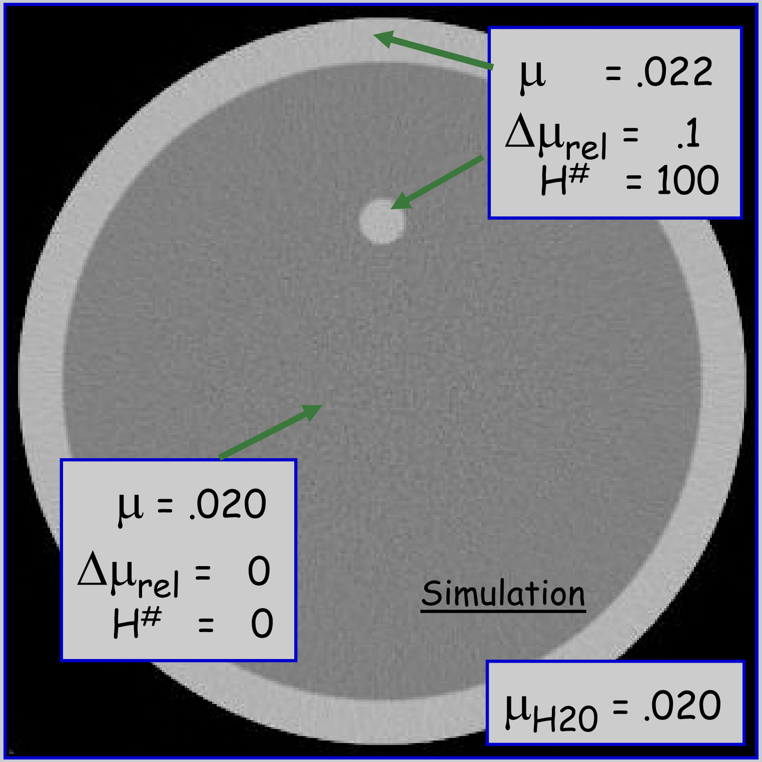

- **Attenuation values:**
  Image reconstruction results in the value for the material attenuation coefficient.

- **Hounsfield Units (HU):**
  Medical standards define the Hounsfield number as the reconstructed attenuation coefficient relative to water,

$$\Delta\mu_{rel}(x,y) = (\mu(x,y) - \mu_{H2O})/\ \mu_{H2O}$$

$$H^{\#} = 1000\ \Delta\mu_{rel}(x,y)$$

$$H^{\#}\ \text{water} = 0$$

$$H^{\#}\ \text{air} = -1000$$

CT numbers for Medical CT images

- For soft tissues, the Hounsfield numbers are between 0 and 100.
- This corresponds to a 1% range of attenuation coefficient values.
- Air (~-1000) and bone (> 1000) provide high contrast.

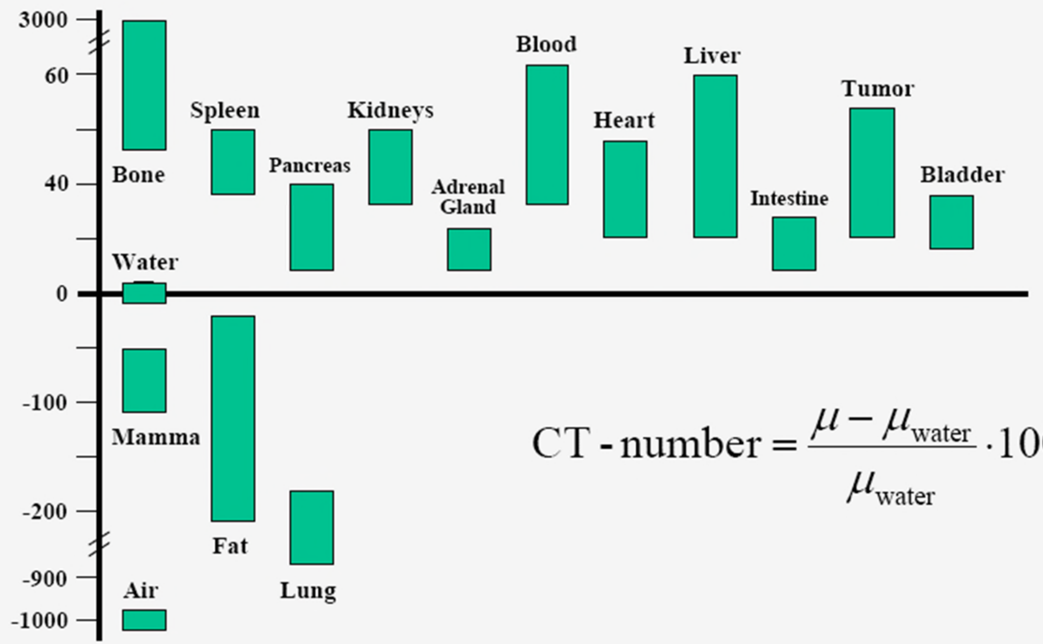

$$\text{CT-number} = \frac{\mu - \mu_{water}}{\mu_{water}} \cdot 1000$$

B) CT Reconstruction

1) Projection geometry
2) Fourier Domain Solution (9 slides)
3) Convolution / Backprojection
4) Cone beam reconstruction
5) Iterative Reconstruction

Theorem first presented in L07

The central slice theorem from Fourier analysis provides a method to easily demonstrate that an object can be reconstructed from projections.

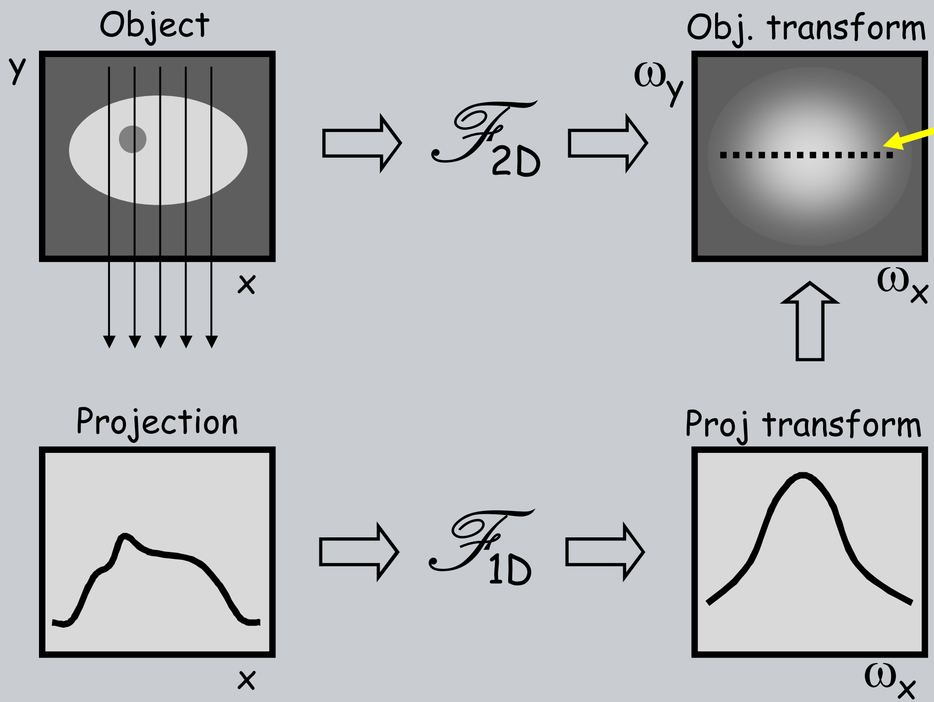

The values of the 1D transform of an object projection are equal to the values of the 2D transform of the object along a line through the (0,0) coordinate that is perpendicular to the projection direction.

Barrett & Swindell, 1981, Pg 384

Theorem first presented in L07

The central slice theorem is easily proven by considering the values of the Fourier transform of an object, ***O(x,y)***, along the $\omega_y = 0$ axis,

$$\Im(\omega_x,\omega_y) = \iint O(x,y)\cdot e^{-2\pi i(\omega_x x+\omega_y y)}dxdy$$

$$\Im(\omega_x,0) = \int\left(\int O(x,y)dy\right)\cdot e^{-2\pi i(\omega_x x)}dx$$

$$\Im(\omega_x,0) = \int\left(P(r,0)\right)e^{-2\pi i(\omega_x x)}dx$$

The inner integration reduces to the projection in a direction parallel to the y axis ($\theta=0$). Other directions can be considered by a simple rotation of the object.

Barrett & Swindell, 1981, Pg 384

VII.B.2 – Fourier reconstruction method.

Projections measured from many directions are transformed to describe the 2D Fourier transform of the object. The Object material properties are estimated using the 2D inverse Fourier transform

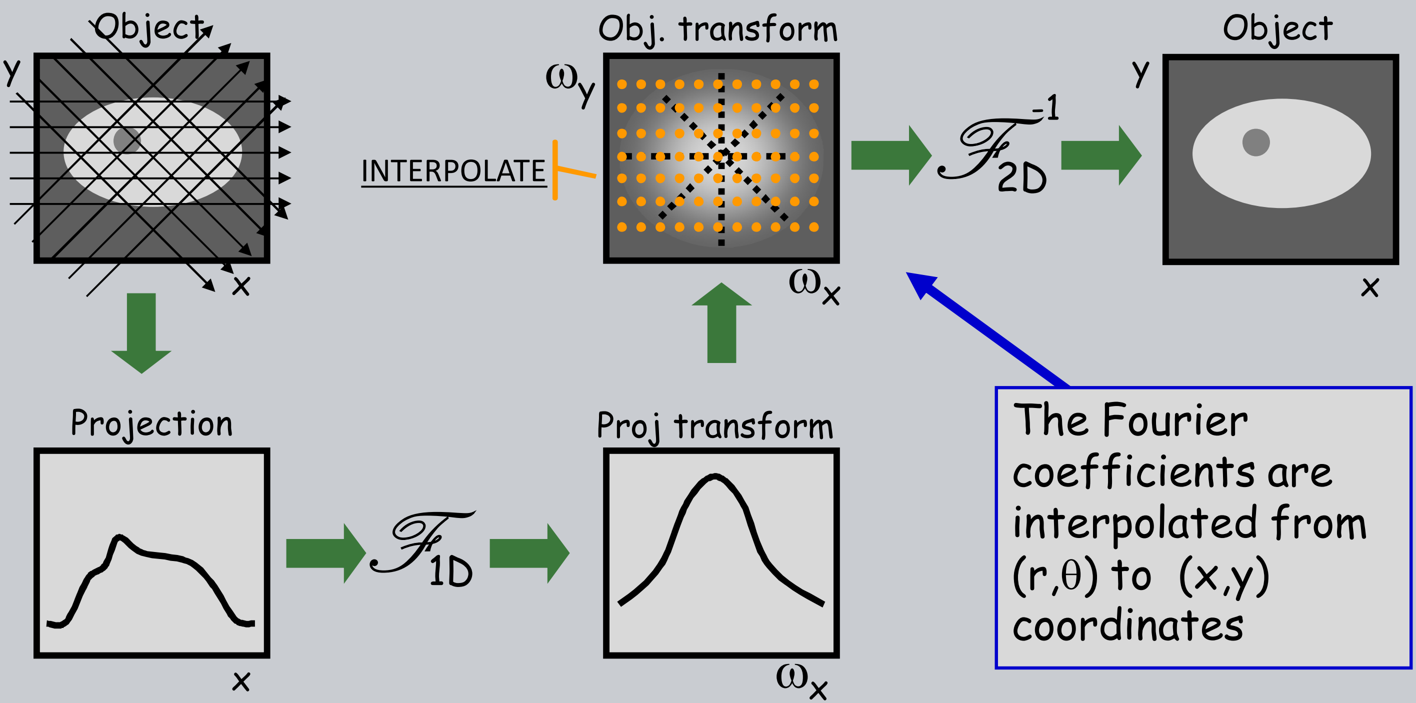

Full sampling of the Fourier domain requires that the radial frequency coefficients be closely spaced in the high frequency portion of the domain.

$\Delta\theta = 2/N$ radians

$N_\theta = \pi/\Delta\theta = N\pi/2$

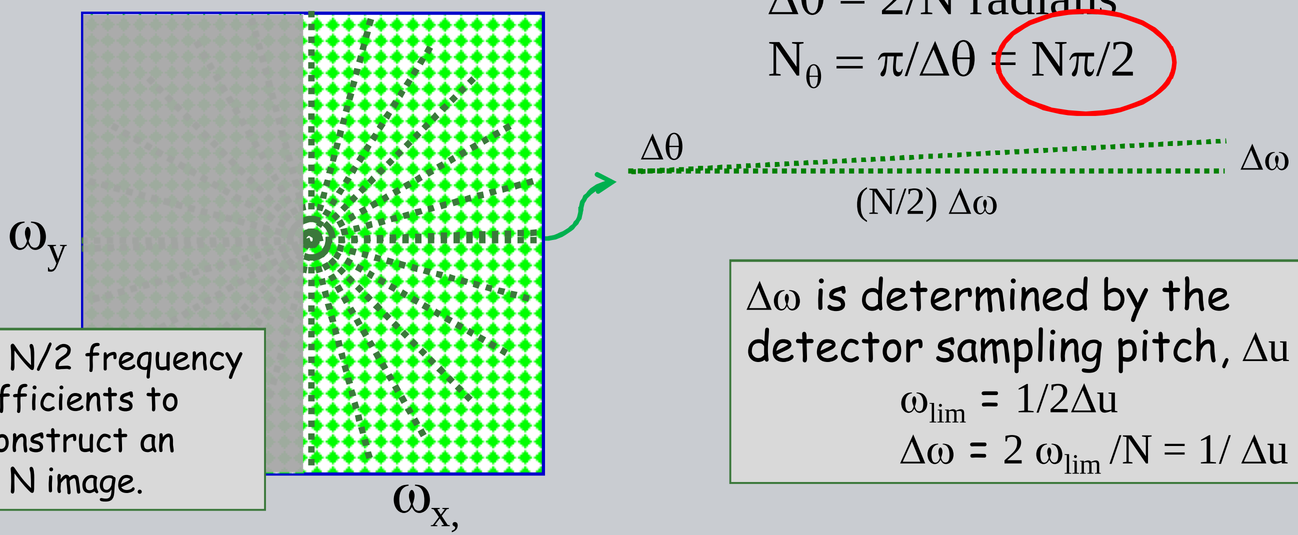

N x N/2 frequency coefficients to reconstruct an N x N image.

$\Delta\omega$ is determined by the detector sampling pitch, Δu .

$\omega_{lim} = 1/2\Delta u$

$\Delta\omega = 2\,\omega_{lim}/N = 1/\Delta u$

Angular sampling may be doubled to overlap the detectors element for each projection sample

Views required to reconstruct a 512x512 image

800 views	180 °	
1600 views	360°	quarter offset geometry
3200 views	360°	¼ offset + double sampling

- Angular sampling over 180 degrees is sufficient to describe an object in the Fourier domain.
- However, 360 degree sampling is commonly done with the rotation center offset by ($\frac{1}{4}$, $\frac{1}{4}$) of the sample increment, $\Delta\mu$.

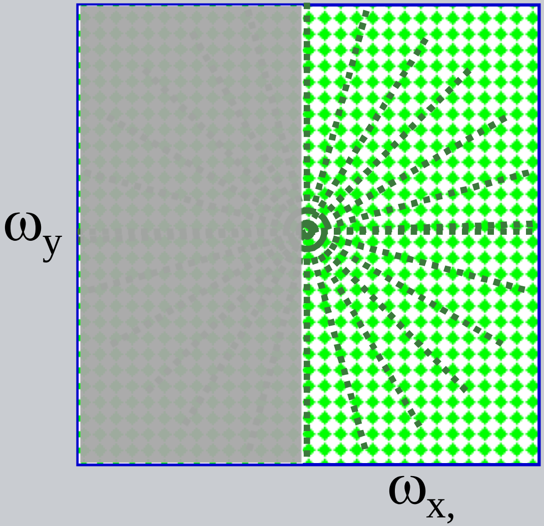

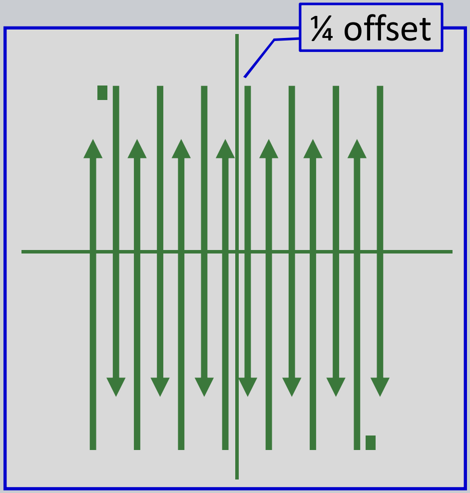

$\frac{1}{4}$, $\frac{1}{4}$ offset sampling improves resolution by decreasing the effective sampling increment , $\Delta\mu$, by a factor of two.

VII.B.2 – Parallel beams, circular orbits

A parallel beam of radiation used to acquire P(u,v) using circular rotational sampling completely samples the 3D Fourier domain.

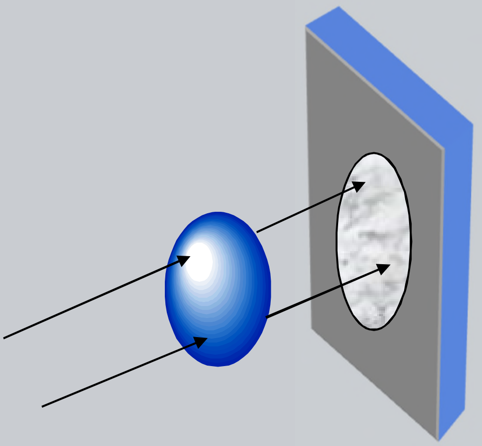

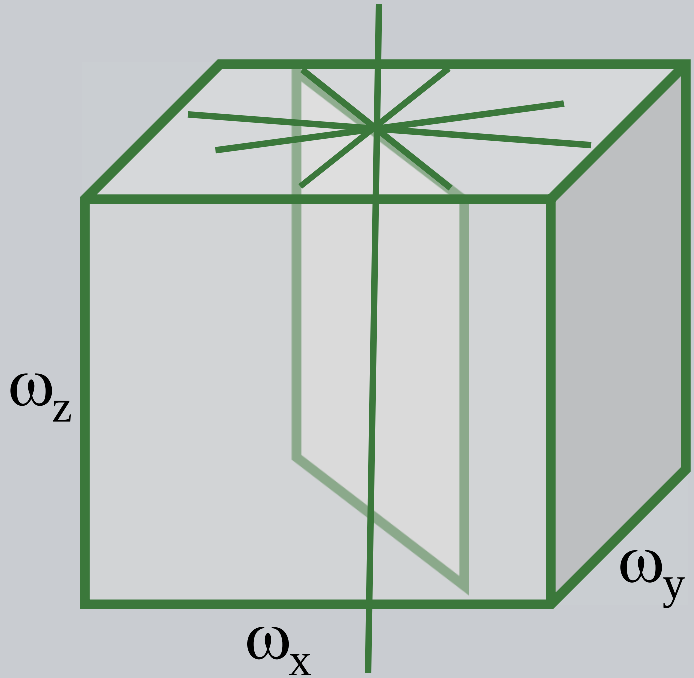

A fan beam of radiation used to acquire P(u) with angular sampling produces frequency samples in the 2D Fourier domain in arcs through the 0,0 axis.

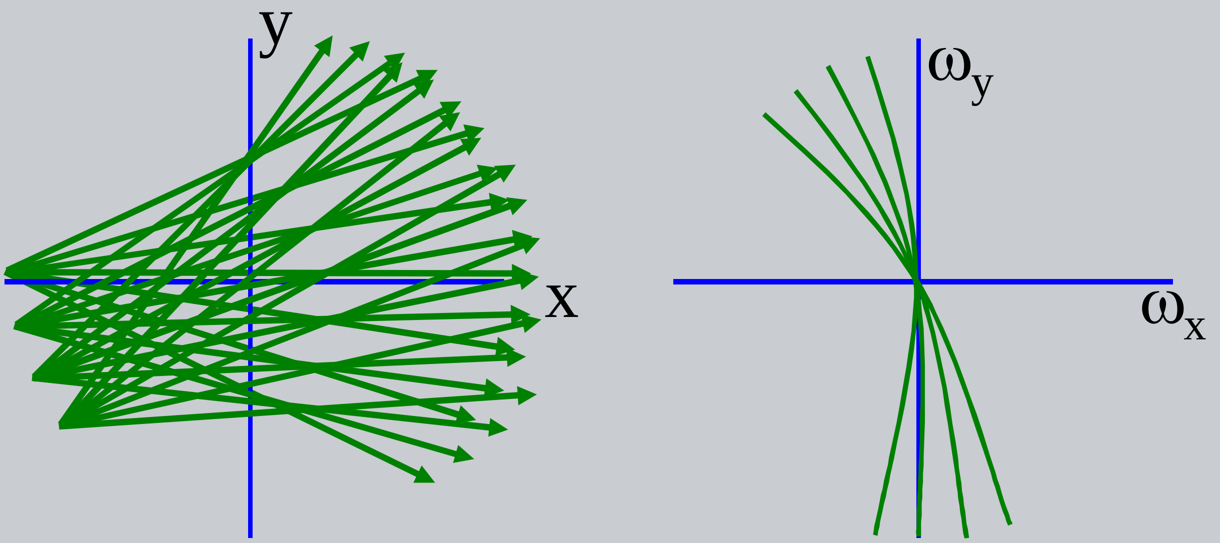

A cone beam of radiation used to acquire P(u,v) with angular sampling DOES NOT FULLY SAMPLE the 3D Fourier domain in the region of the axis.

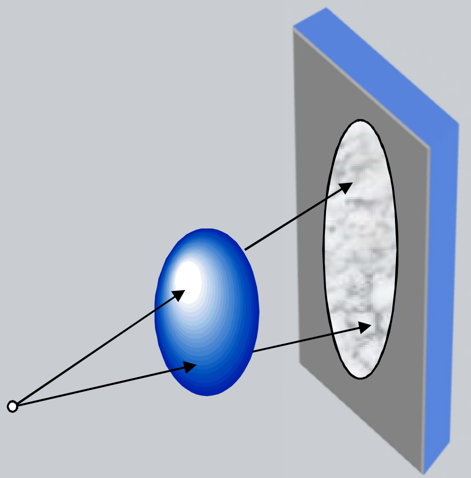

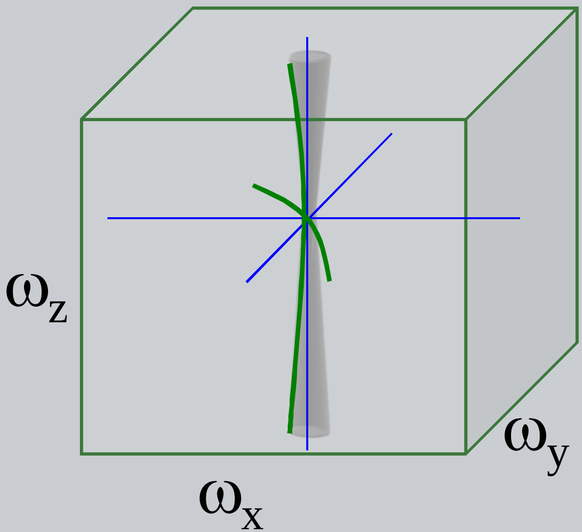

Each projection is associated with a dish shaped surface of fourier coefficients going through the 3D frequency domain. When rotated, there is a void of coefficients along the axis of rotation.

- The Radon values of all planes intersecting the object have to be known in order to perform an exact reconstruction. The Tuy sufficiency condition (Tuy 1983) states that exact reconstruction is possible if all planes intersecting the object also intersect the source trajectory at least once.
- The circular trajectory does not satisfy the Tuy-Smith condition as illustrated. It is therefore necessary to extend the trajectory with an extra circle or line if exact reconstruction is required.

Tuy, H. (1983). An inversion formula for cone-beam reconstruction. *SIAM Journal of Applied Mathematics 43*, 546–552.

B) CT Reconstruction

1) Projection geometry
2) Fourier Domain Solution
3) Convolution / Backprojection (11 slides)
4) Cone beam reconstruction
5) Iterative Reconstruction

From: impactscan.org

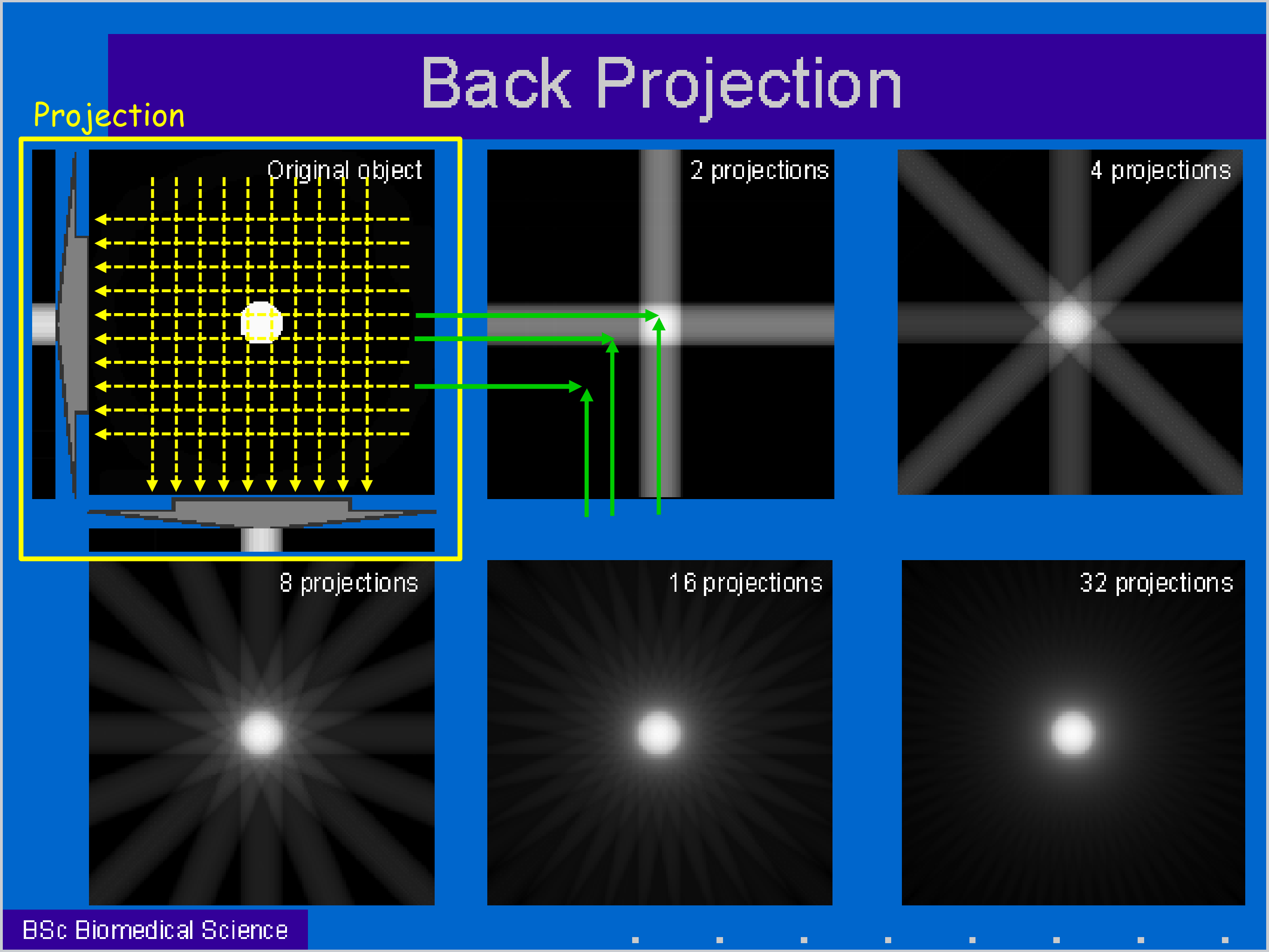

From: impactscan.org

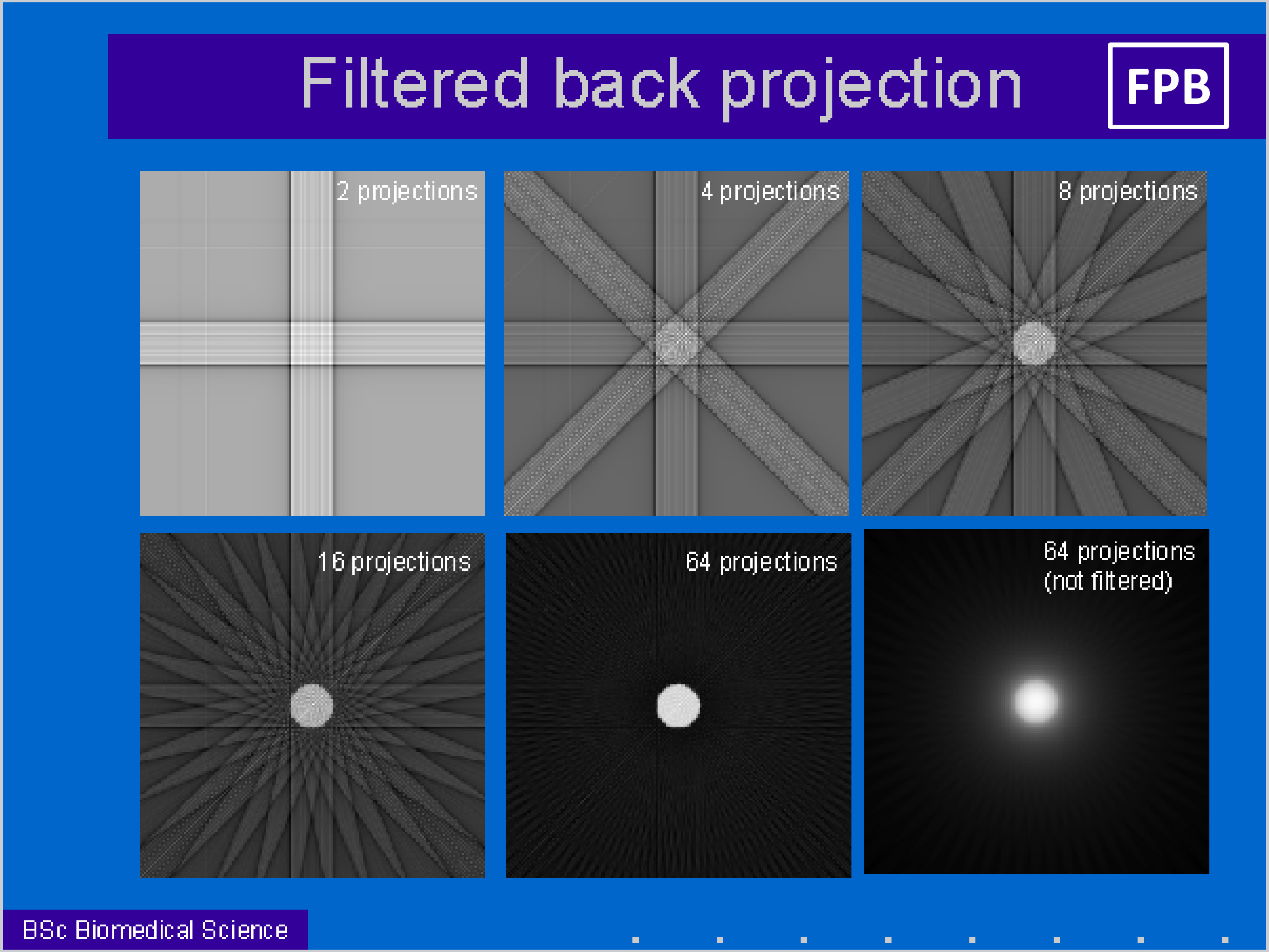

Filtered – Backprojection

1. Measure projections.
2. Filter projections.
3. Backproject.

   For every point in the reconstruction image, the value for each filtered projection is interpolated and added to the the image.

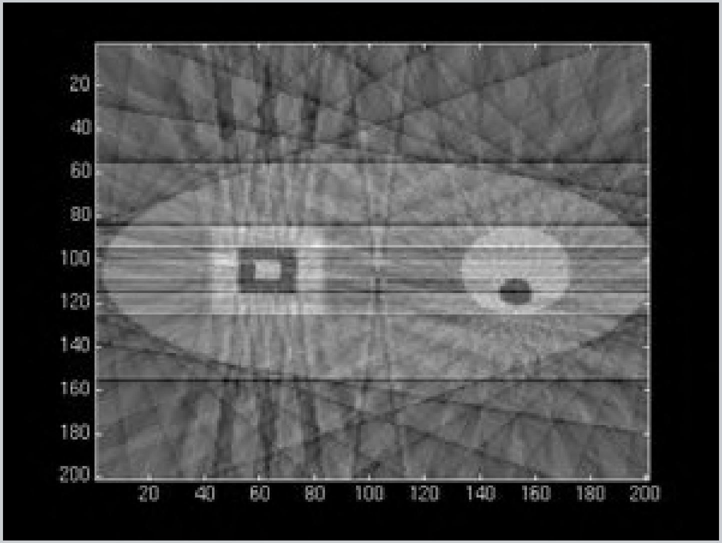

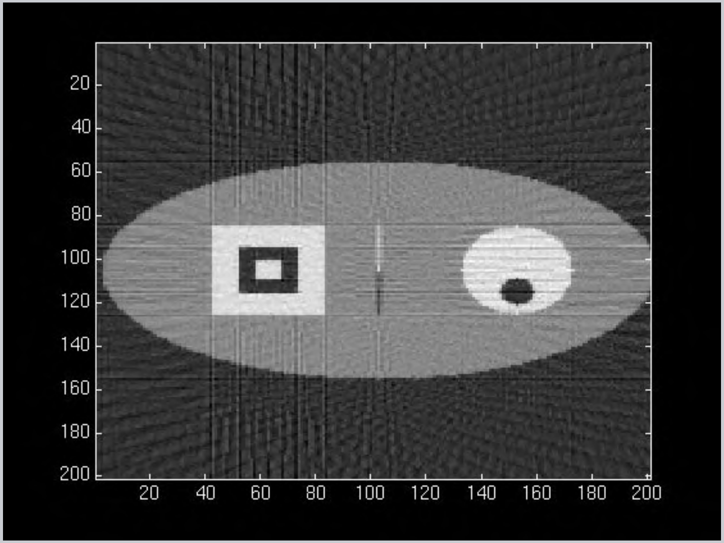

Projections are filtered either by

- convolution with a spatial kernel or
- Fourier transformations with a filter function

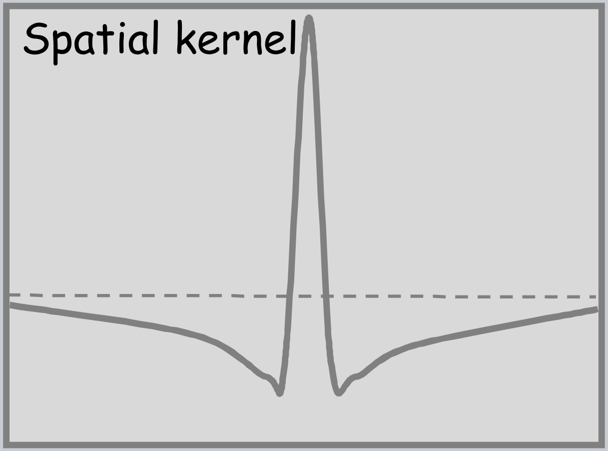

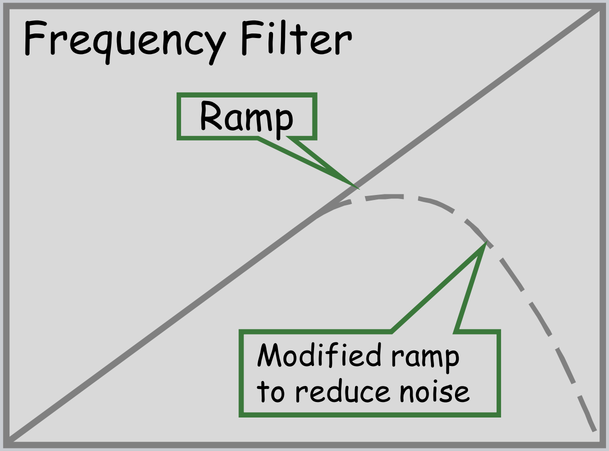

Equivalent:

- Convolution Backprojection
- Filtered Backprojection

VII.B.3 – Discrete kernals/filters

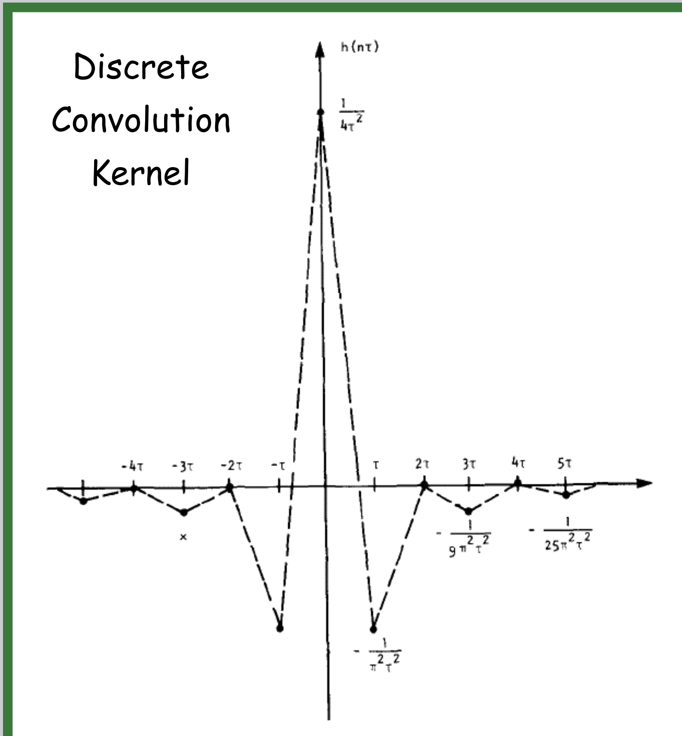

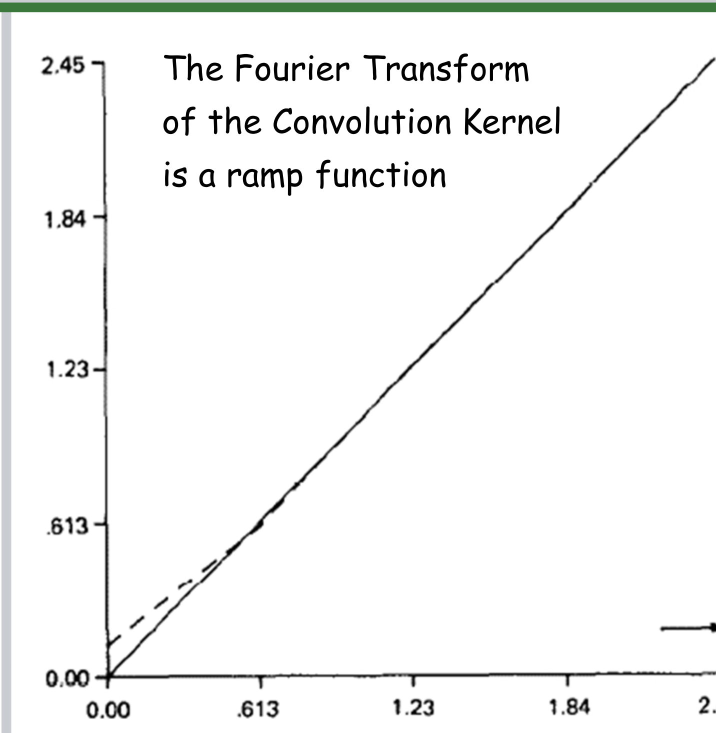

- A. C. Kak and Malcolm Slaney,
  Principles of Computerized Tomographic Imaging, IEEE Press, 1988.
- http://www.slaney.org/pct/pct-toc.html

VII.B.3 – Modified filters

The ideal filter (ramp) is usually modified to smooth noise or sharpen edges.

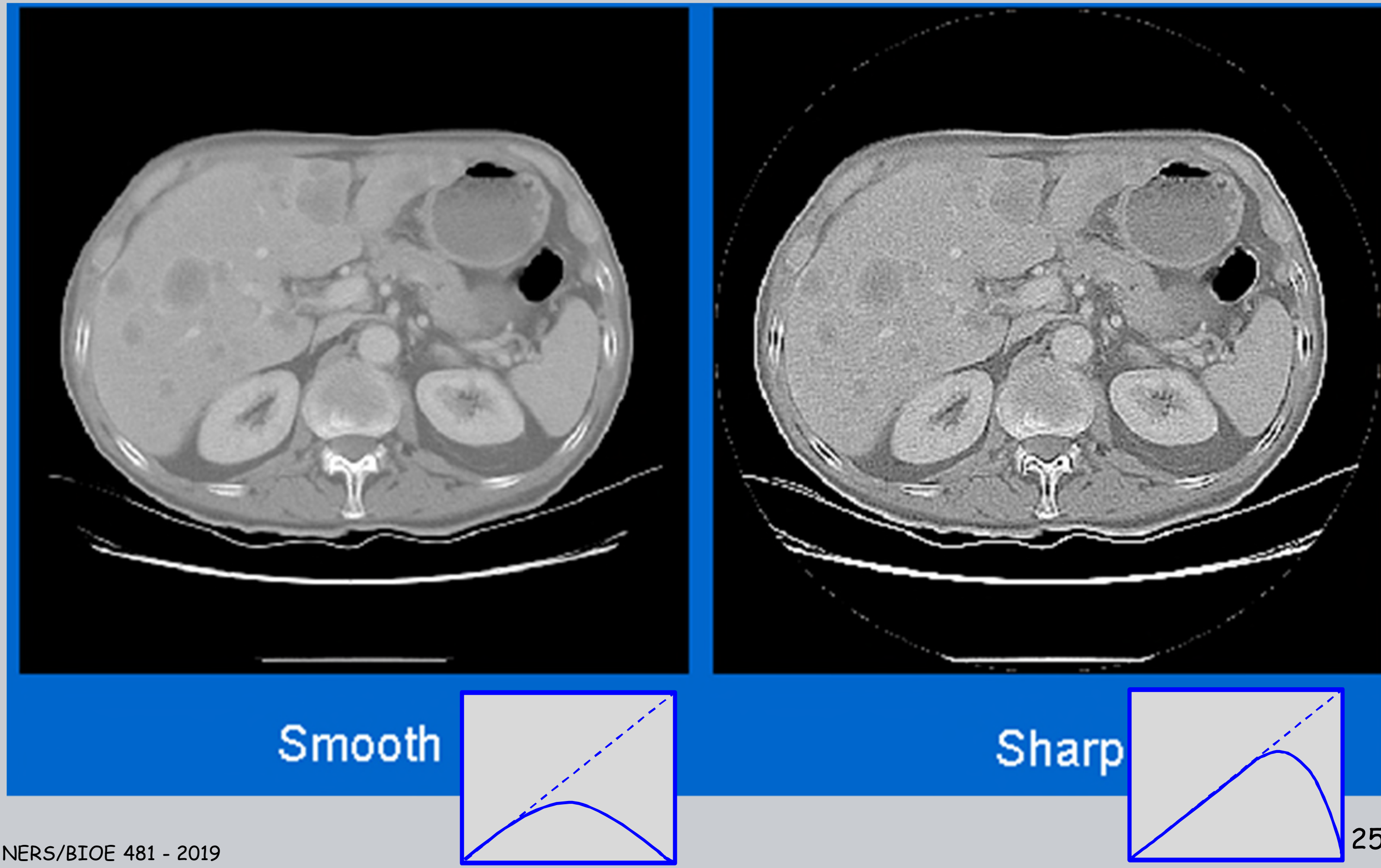

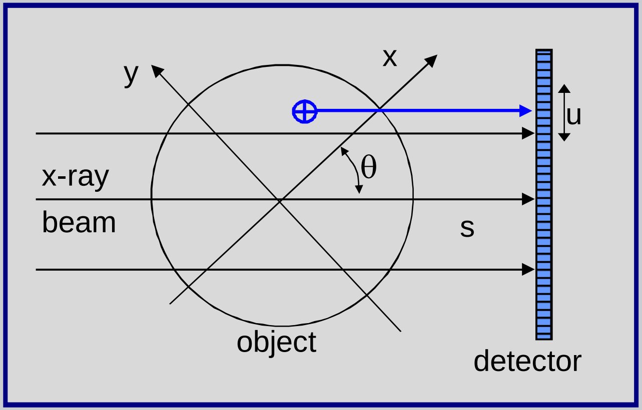

- Consider *(x,y)* positions in a plane of an object rotated about the *z* axis thru θ degrees.
- The projection thru this point to the position *u* on the detector is,

$$P(u,\theta) = \int \mu(s)ds$$

$$u(x,y,\theta) = x\sin(\theta) + y\cos(\theta)$$

For each point *(x,y)* , the value of μ is equal to the integral of the convolved projection over all angles

where;

- $u = u(x,y,\theta)$
- The convolution Kernal is the inverse Fourier transform of the ramp function, $|\omega|$, and any addition smoothing filter, $F(\omega)$.

$$\mu(x,y) = \int P^*(u,\theta)d\theta$$

$$P^*(u,\theta) = P(u,\theta) * K(u)$$

$$= \int K(u'-u)P(u',\theta)du'$$

$$K(u) = \int F(\omega)|\omega|e^{i\omega u}d\omega$$

VII.B.3 – FBP reconstruction, 2D parallel, discrete notation

- For a detector with discrete elements spaced at a distance of Δu , the convolution can be written as a sum over the discrete kernel.
- While this sum is written with infinite limits, it is bounded by the object beyond which P is zero.
- The reconstruction can be similarly written as a discrete sum with a constant corresponding to the angular range.

$$P^*(u,\theta_k) = \sum_{l=-\infty}^{+\infty} K(l\Delta u - u) P(l\Delta u, \theta_k)\Delta u$$

$$\mu(x,y) = \frac{\pi}{N_\theta}\sum_{k=1}^{N_\theta} P^*(u,\theta_k)$$

If we write the solution as a double sum for the convolution and the backprojection, we can see that the noise of the results will be determined by the noise in the projection values at each position and angle.

$$\mu(x,y) = \frac{\pi}{N_\theta}\Delta u \sum_{k=1}^{N_\theta}\sum_{l=-\infty}^{+\infty} K(l\Delta u - u) P(l\Delta u, \theta_k)$$

$$\sigma^2_{\mu(x,y)} = \left\{\frac{\pi}{N_\theta}\Delta u\right\}^2 \sum_{k=1}^{N_\theta}\sum_{l=-\infty}^{+\infty} \{K(l\Delta u - u)\}^2 \sigma^2_{P(l\Delta u,\theta_k)}$$

VII.B.3 – FBP reconstruction, 2D parallel, discrete notation

- A useful solution for the noise in a reconstruction can be found for the special case of a cylindrical homogenous object.
- We then consider only the noise of the reconstruction in the center which is influenced by the noise in the central ray projection, P_0.
- The central ray projections are rotationally similar with a noise of σ_P .

Note: The fan beam solution (central cone) is the same as the parallel beam for the central ray (see VII.B.4).

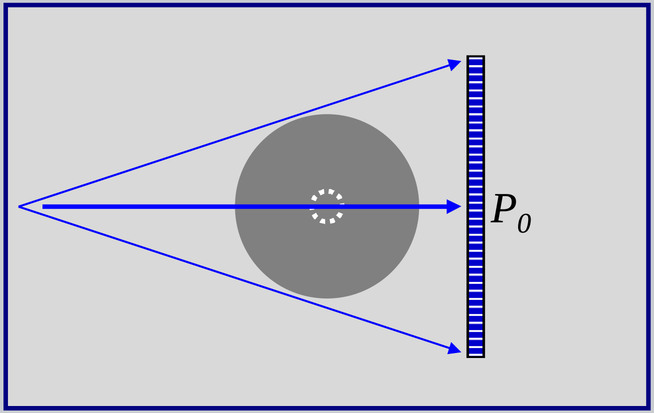

- If the projection noise does not vary with angle, σ_P , then projection variance, $\sigma_P{}^2$, can be taken out of the summations.
- The angular summation is now trivial and results in an N_θ term that cancels one in the denominator.

$$\sigma^2_{\mu(x,y)} = \frac{\{\pi \Delta u\}^2}{N_\theta} \alpha^2 \sigma^2_P$$

$$\alpha^2 = \sum_{l=-\infty}^{+\infty} \{K(l\Delta u - u)\}^2$$

VII.B.3 – FBP reconstruction, 2D parallel, discrete notation

- A common smoothing function used to modify the ramp filter is the sinc function, $sin(\omega)/\omega$.
- For this the α^2 term is a function of the limiting spatial frequency,

$$\omega_{lim}=1/(2\Delta u)$$

Note: See the lecture notes on CT noise propogation for the derivation of α^2 .

sinc filter

$$\alpha^2 = \frac{\omega_{\lim}^2}{2\pi^2}$$

$$\sigma_\mu^2 = \frac{\omega_{\lim}^2}{2N_\theta}\sigma_P^2 = \frac{1}{2^3 N_\theta (\Delta u)^2}\sigma_P^2$$

We recall now that the Projection is proportional to the natural log of the detected signal and thus the projection noise is equal to the relative noise of the detector signal.

$$P = -ln(S/S_o) = ln(S_o) - ln(S)\ , \quad \sigma_P=\sigma_S/S$$

In terms of the noise equivalent quanta, Qeq , the projection noise is thus,

$$\sigma_P{}^2= 1/SNR^2 = 1/(\ Q_{eq} A_d) = 1/(\ Q_{eq}\ \Delta u\ S_w)$$

where A_d = detector area, S_w = slice width.

sinc filter

$$\sigma_\mu^2 = \frac{1}{2^3 N_\theta (\Delta u)^3 S_w}\left(\frac{1}{Q_{eq}}\right)$$

Note:

- For cone beam CT, $S_w = \Delta u$, and the CT noise is inversely proportional to the pixel area.
- Noise is inversely proportional to (mas)$^{1/2}$ due to Qeq.
- CT SNR = μ / σ_μ

- The Noise Power Spectrum (NPS) for CT reflects the modified ramp function used to filter the projections.
- As expected, the variance of reconstructed image values will be proportional to the area under the NPS.

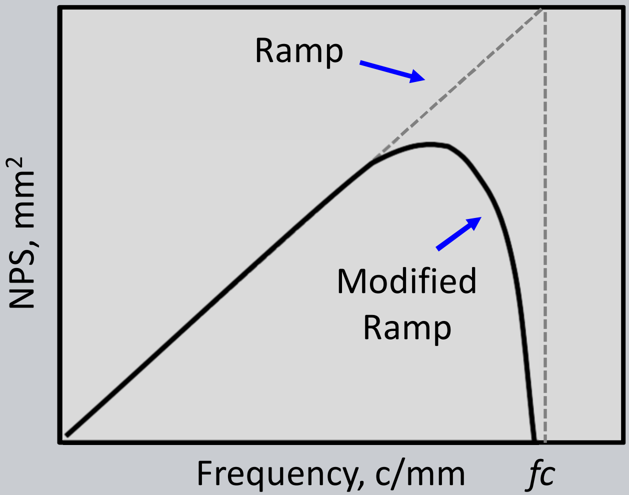

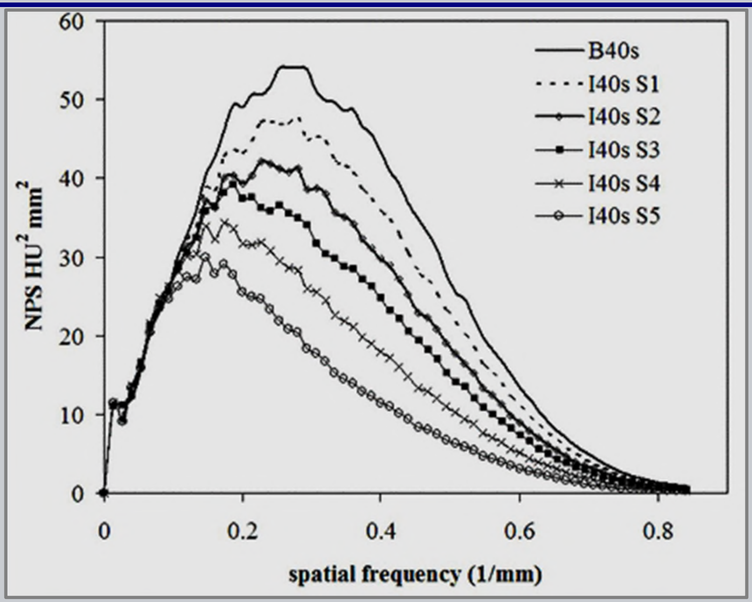

Ghetti2013, JACMP

NPS measured for a SOMATOM Definition Flash CT scanner (Siemens).

- B40s is a standard FBP filter.
- I40s S[1-5] are filters used with the SAFIRE reconstruction algorithm.

B) CT Reconstruction

1) Projection geometry
2) Fourier Domain Solution
3) Convolution / Backprojection
4) Cone beam reconstruction (11 slides)
5) Iterative Reconstruction

VII.B.4 – FDK – Feldkamp, Davis, Kress

FDK

Practical cone-beam algorithm

L. A. Feldkamp, L. C. Davis, and J. W. Kress

Research Staff, Ford Motor Company, Dearborn, Michigan 48121

Received November 11, 1983; accepted February 28, 1984

The cone-beam reconstruction algorithm developed at FMC is still widely used for both laboratory and clinical systems. The original paper has been cited over 5000 times (google scholar, 2017)

The original mCT system from Ford Motor Co.

Fein Focus source

Image intensifier

(relocated to HFHS)

VII.B.4 – Geometry nomenclature

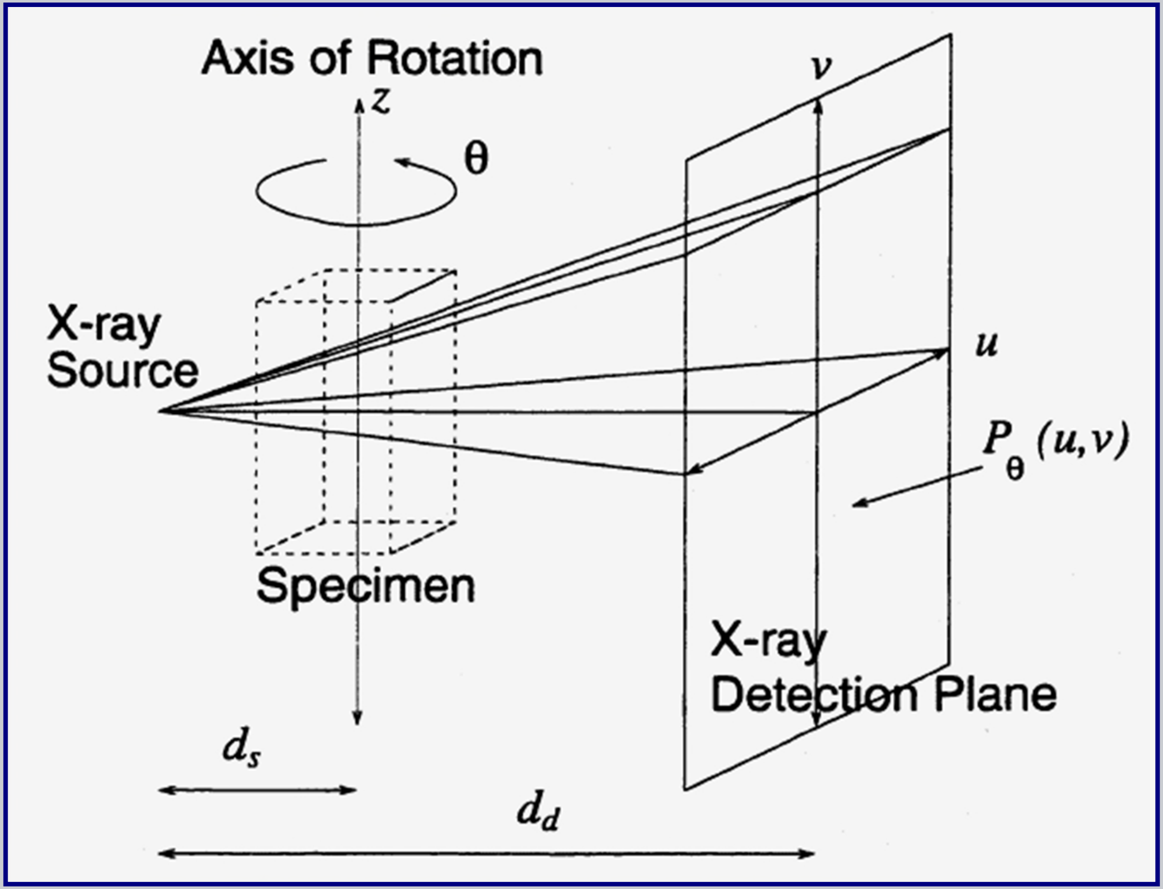

Reimann, WSU thesis, 1998

- A 3D solution for a parallel beam is a simple extension of the 2D solution.
- Each plane is an independent 2D solution.

- Resample detector data for alignment with rotation axis

$$P_\theta(u,v)$$

- Convolve the Projection Data in the direction of rotation

$$P_\theta^*(u,v) = P_\theta(u,v) * h(u)$$

- Backproject the convolved Projection Data

$$\mu(x,y,z) = \int_0^{2\pi} P_\theta^*(x',z')\,d\theta$$

The Feldkamp solution weights the projection data and scales the backprojection

- Weight Projection Data

$$P_\theta^{'}(u,v) = \frac{d_s}{\sqrt{d_s^2 + v^2 + u^2}} P_\theta(u,v)$$

- Convolve Weighted Projection Data

$$P_\theta^{*}(u,v) = P_\theta^{'}(u,v) * h(u)$$

- Backproject the convolved weighted Projection Data

$$\mu(x,y,z) = \int_0^{2\pi} \frac{d_s^2}{(d_s - y)^2} P_\theta^{*}\left(\frac{d_s x'}{d_s - y'}, \frac{d_s z'}{d_s - y'}\right) d\theta$$

VII.B.4 – FKD pseudocode A – process the projection views

for each vertical detector position v (N_v positions):
  for each horizontal detector position u (N_u positions):
    precompute weights $w(u, v) = d_s / \sqrt{d_s^2 + u^2 + v^2}$
  end u loop
end v loop

for each θ (N_θ views):
  Weight Projection
  for each vertical detector position v (N_v positions):
    for each vertical detector position u (N_u positions):
      $p'_\theta(u, v) = p_\theta(u, v) w(u, v)$
    end u loop
  end v loop

  Fourier Filter Zero Padded Projections 2 rows at a time
  for every other vertical detector position v ($N_v/2$ positions):
    $P(u) = FFT\{p'_\theta(u, v)$ and $p'_\theta(u, v+1)\}$
    for each zero padded horizontal detector position u ($2N_u$ positions):
      $P^*(u) = P(u)h(u)$
    end u loop
    $p^*_\theta(u, v)$ and $p^*_\theta(u, v+1) = FFT^{-1}\{P^*(u)\}$
  end v loop

VII.B.4 – FKD pseudocode B - Backproject

for each y position (N_y positions):

  for each x position (N_x positions):

    compute $x' = x\cos\theta + y\sin\theta$

    compute $y' = y\cos\theta - x\sin\theta$

    compute $M = d_s/(y' - d_s)$

    compute $u = x'M + u_0$

    compute M^2

    compute $M^2 c_2 = M^2(\lfloor u \rfloor)$

    compute $M^2 c_1 = M^2(1 - \lfloor u \rfloor)$

    For each z position (N_z positions):

      compute $v = zM + v_0$

      compute $c_4 = \lfloor v \rfloor$

      compute $c_3 = 1 - \lfloor v \rfloor$

      interpolate $M^2 p^*_\theta(u,v) = c_4(c_2 P(\lfloor u+1 \rfloor, \lfloor v+1 \rfloor)$
        $+ c_1 P(\lfloor u \rfloor, \lfloor v+1 \rfloor)) + c_3(c_2 P(\lfloor u+1 \rfloor, \lfloor v \rfloor) + c_1 P(\lfloor u \rfloor, \lfloor v \rfloor))$

      increment $I(x,y,z)$ by $M^2 p^*_\theta(u,v)$

      end z loop

    end x loop

  end y loop

end θ loop

Backproject each view column by column.

VII.B.4 – FKD pseudocode, C computation overhead

Line Number	Floating Point Operations Required per Step	Total Times Step is Executed	Total Floating Point Operations Required
3	7	$N_v N_u$	$7N_v N_u$
11	1	$N_\theta N_v N_u$	$N_\theta N_v N_u$
17	$9(2N_u \log_2(2N_u))$	$N_\theta(N_v/2)$	$9N_\theta N_v N_u \log_2(2N_u)$
19	2	$N_\theta(N_v/2)(2N_u)$	$2N_\theta N_v N_u$
21	$9(2N_u \log_2(2N_u))$	$N_\theta(N_v/2)$	$9N_\theta N_v N_u \log_2(2N_u)$
26	3	$N_\theta N_y N_x$	$3N_\theta N_y N_x$
27	3	$N_\theta N_y N_x$	$3N_\theta N_y N_x$
28	2	$N_\theta N_y N_x$	$2N_\theta N_y N_x$
29	2	$N_\theta N_y N_x$	$2N_\theta N_y N_x$
30	1	$N_\theta N_y N_x$	$N_\theta N_y N_x$
31	1	$N_\theta N_y N_x$	$N_\theta N_y N_x$
32	2	$N_\theta N_y N_x$	$2N_\theta N_y N_x$
34	2	$N_\theta N_z N_y N_x$	$2N_\theta N_z N_y N_x$
36	1	$N_\theta N_z N_y N_x$	$N_\theta N_z N_y N_x$
37	8	$N_\theta N_z N_y N_x$	$8N_\theta N_z N_y N_x$
38	1	$N_\theta N_z N_y N_x$	$N_\theta N_z N_y N_x$

The heavy lifting is in the column backprojection

To reconstruct an N x N x N volume,

$$N_\theta = N\pi/2$$

$$FLOPS = N^4 6\pi + \delta$$

Thus,

$$512^3 \rightarrow 1300 \times 10^9 \ FLOPS$$

FLOPS – Floating Point Operations Per Second

3 GHz Xeon processors are rated by Intel at 50 GFLOPS.

However, for reconstruction problems speed is often limited by memory i/o rates.

VII.B.4 – FKD pseudocode, C computation overhead

N	64	128	256	512	1024
Trad.	$1 \cdot 10^8$	$2 \cdot 10^9$	$3 \cdot 10^{10}$	$5 \cdot 10^{11}$	$9 \cdot 10^{12}$
Fast	$2 \cdot 10^8$	$2 \cdot 10^9$	$2 \cdot 10^{10}$	$2 \cdot 10^{11}$	$1 \cdot 10^{12}$

Table 3.4 *Number of FLOPs on projection data in traditional and fast backprojection as a functrion of* $N = N_x = N_y = 2N_z = N_t = N_q = N_\theta/2$. *The estimate for fast backprojection when* $N = 1024$ *is extrapolated.*

- Henrik Turbell, Cone-Beam Reconstruction Using Filtered Backprojection, PhD Dissertation no. 672, Linkoping University, Sweden, February, 2001
- http://www.cvl.isy.liu.se/ScOut/Theses/

VII.B.4 – HFHS animal femur mCT

1500 x 1500 x 1250

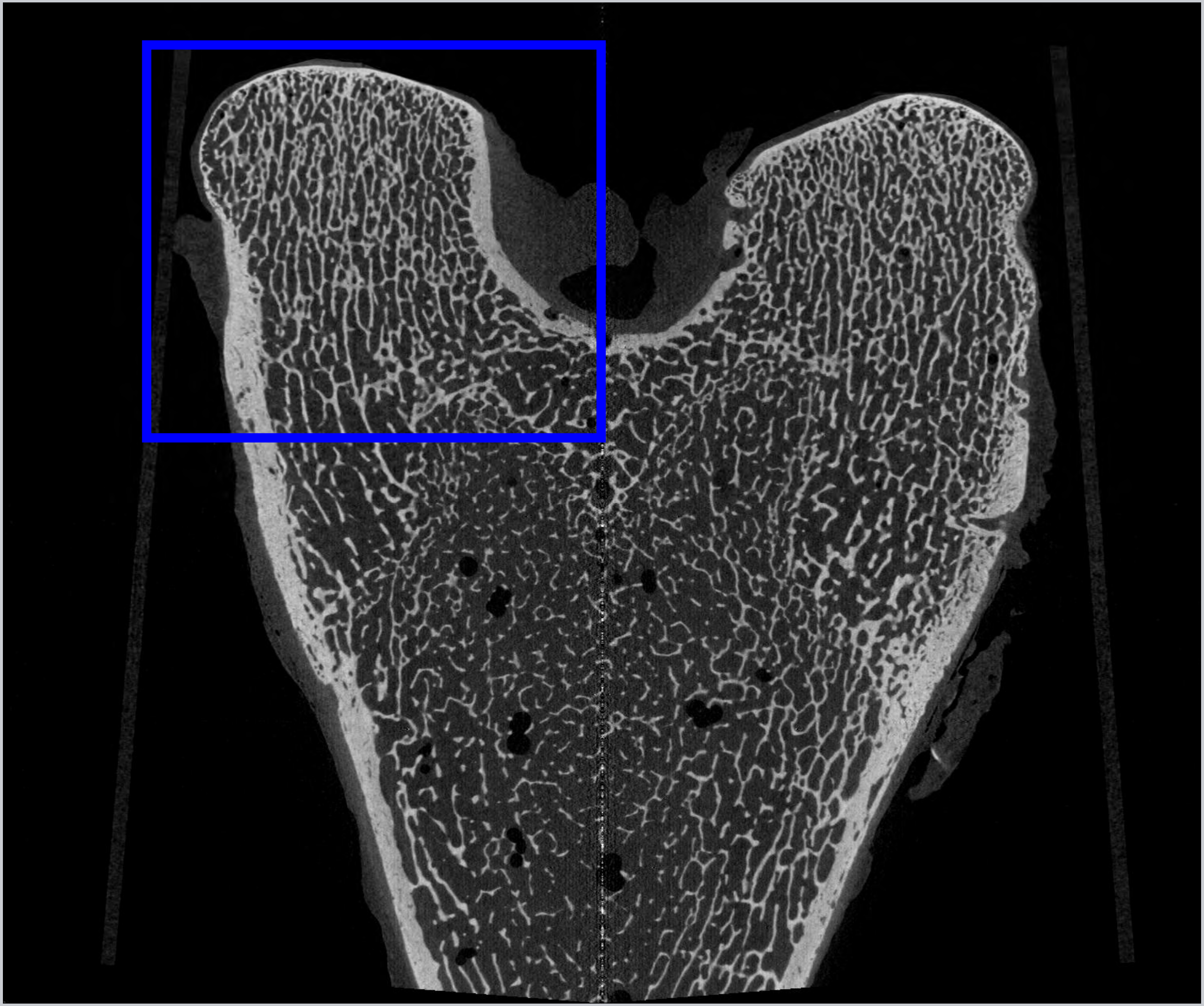

VII.B.4 – HFHS femur mCT

ZOOM

- 1536 x 1920 Acq.
  PaxScan 2520
- Cubic spline resample
  Thevenaz, 'interpol'
- Compress proj data
  JPEG2000 8-1
  Kakadu
- Filtered Backproj.
  MPI cluster (6/12)
- DICOM VCT data
  JPEG2000 8-1
  DCMTK (OFFIS)

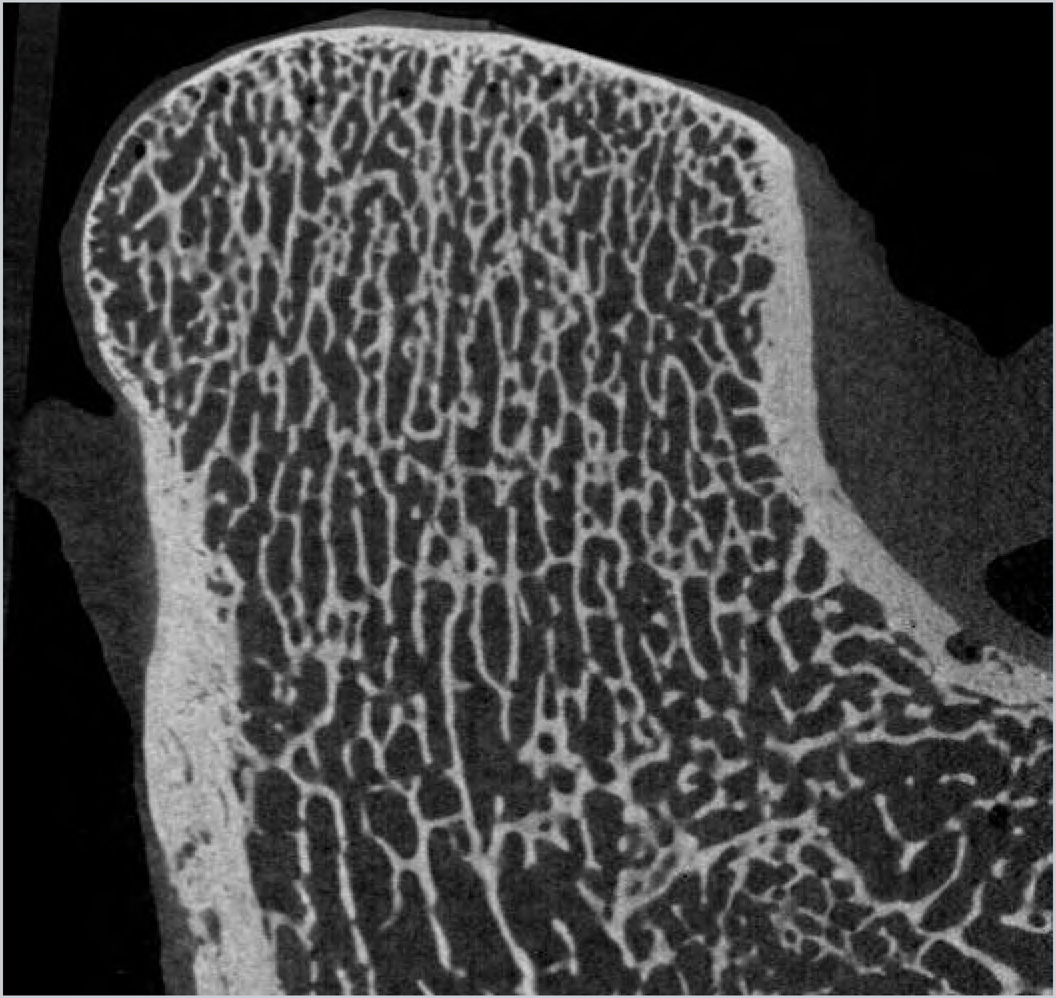

B) CT Reconstruction

1) Projection geometry
2) Fourier Domain Solution
3) Convolution / Backprojection
4) Cone beam reconstruction
5) Iterative Reconstruction (9 slides)

VII.B.5 – Iterative Reconstruction

In general, iterative reconstructions make an initial guess as to the tomographic solution, then

- reproject in a particular direction
- examine the difference between the reprojected estimate and an actual measurement.
- distribute the difference back to the solution estimate

Consider the simple example from the Webb reading assignment where a 3 x 3 tomograph is considered.

- The actual object has values from 1 to 9.
- 4 projection measurements are made.

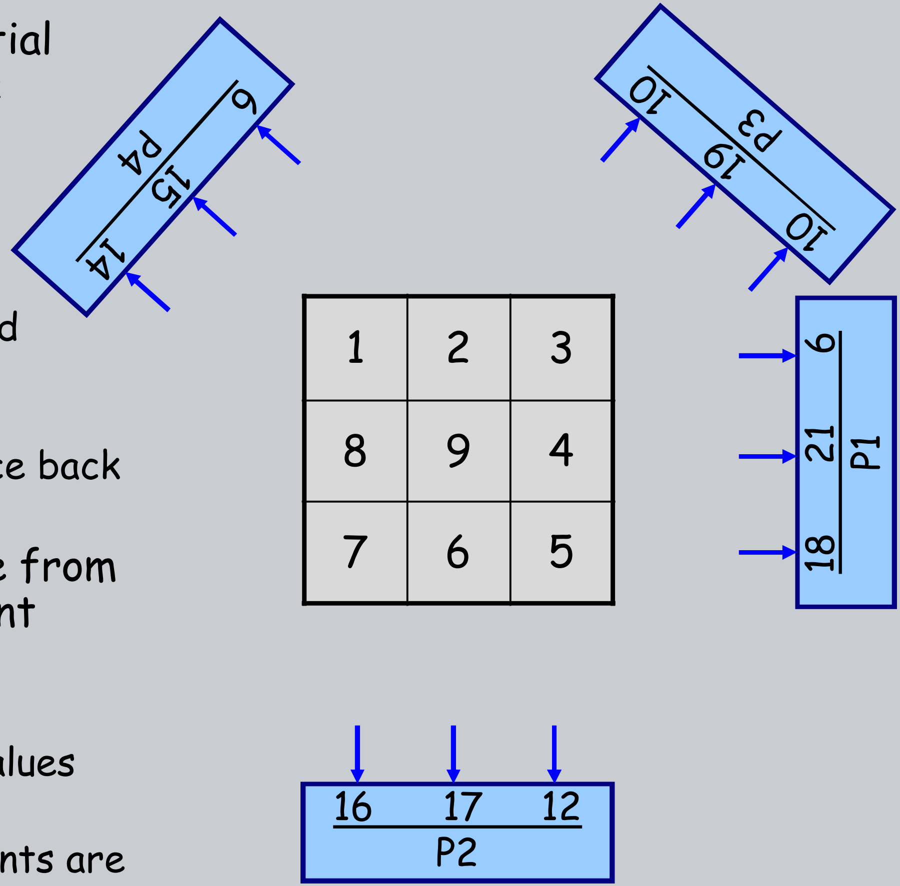

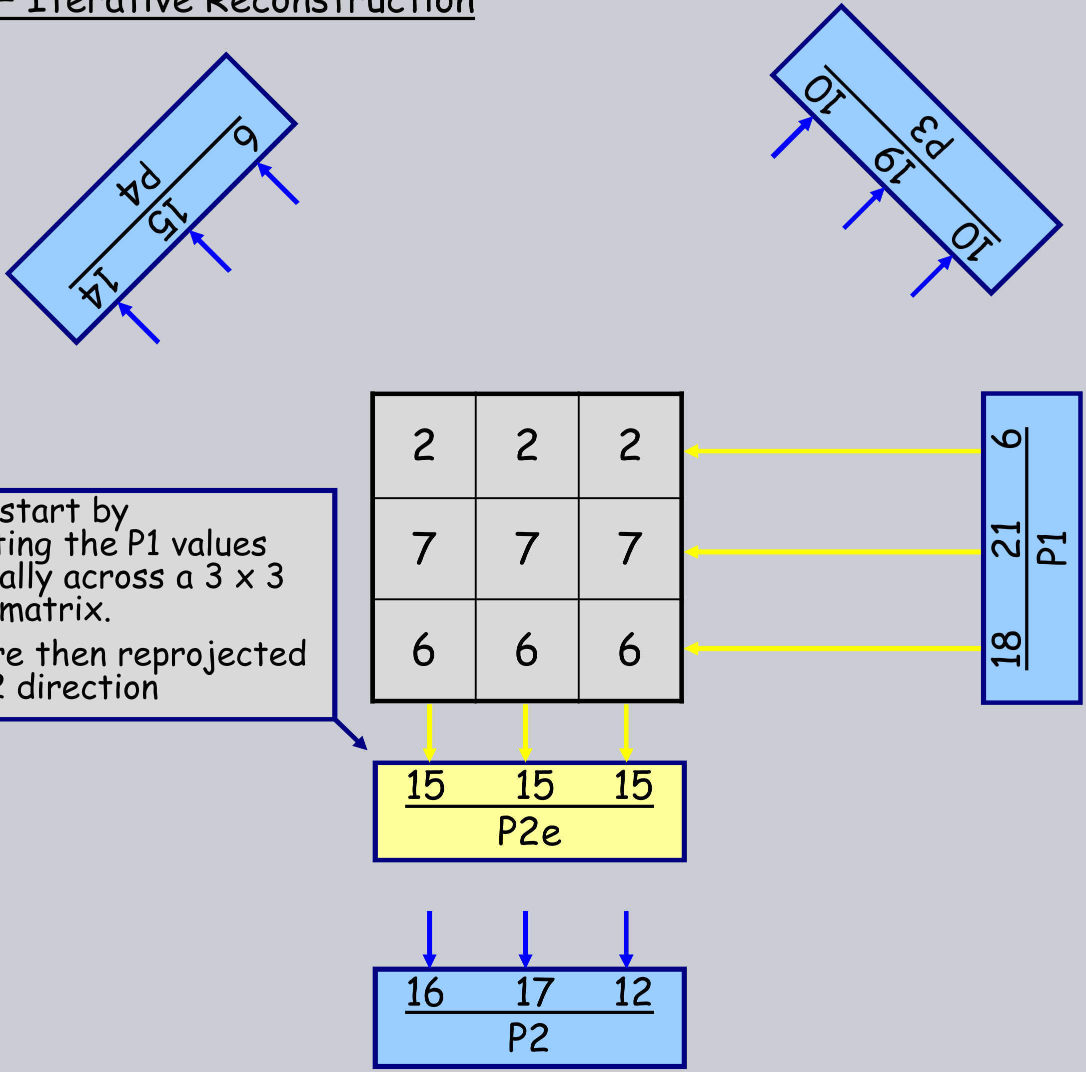

- We now start by distributing the P1 values horizontally across a 3 x 3 solution matrix.
- These are then reprojected in the P2 direction

VII.B.5 – Iterative Reconstruction

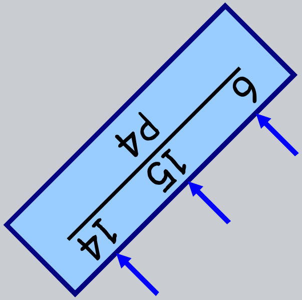

- We then take the difference between the original projection, P2, and the estimate, P2e, and backproject it to get a second estimate.
- The is then reprojected in the P3 direction.

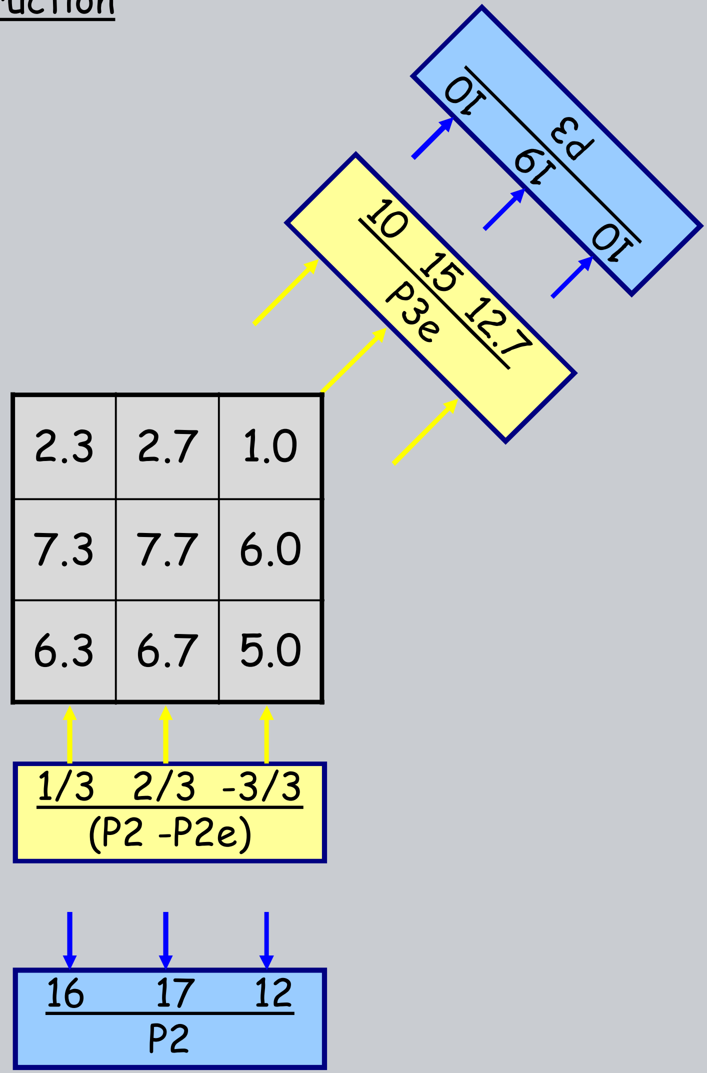

VII.B.5 – Iterative Reconstruction

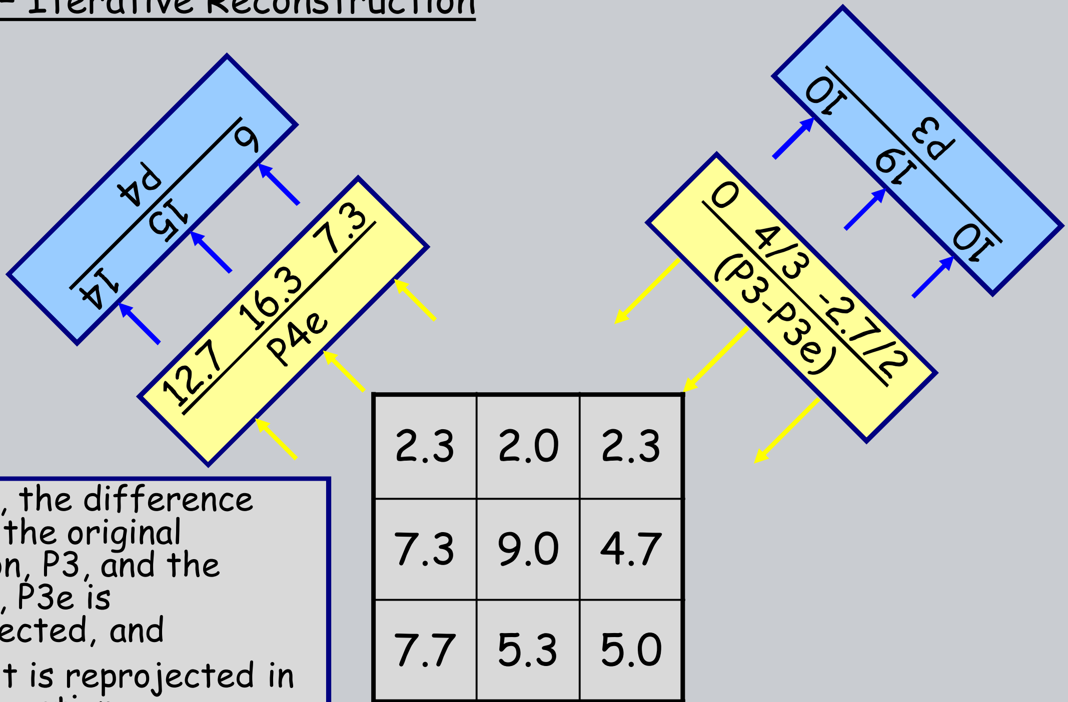

- Similarly, the difference between the original projection, P3, and the estimate, P3e is backprojected, and
- the result is reprojected in the P4 direction.

VII.B.5 – Iterative Reconstruction

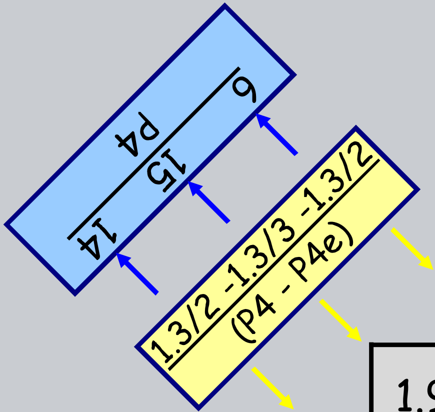

1.9	2.1	2.3
8.0	8.6	4.0
7.7	6.0	4.6

- Finally, the difference between the original projection, P4, and the estimate, P4e is backprojected.
- the result after 1 iteration closely approximates the original values.

Original

1	2	3
8	9	4
7	6	5

VII.B.5 – Maximum Liklihood CT reconstruction

- Maximum Liklihood (ML) reconstruction methods offers the possibility to include the Poisson statistics of the photons in the reconstruction. Since the projections, i, are independent, the log-likelihood, L, can be written as,

$$L = \sum_i \left(- d_i e^{-\sum_j A_{ij}\mu_j} - Y_i \sum_j A_{ij}\mu_j \right) + c_1$$

Equation 5
Ziegler 2007

- where
  - di is the expected number of photons leaving the source along the ith projection,
  - Yi are the observed photon counts along projection i,
  - μ_j is the absorption coefficient of the jth supporting grid point,
  - Aij are the elements of the system matrix, and c1 is an irrelevant constant
- An approximate solution of maximizing L leads to an iterative step n to n+1 of,

$$\mu_j^{n+1} = \mu_j^n + \mu_j^n \frac{\sum_i A_{ij}[d_i e^{-\langle A_i, \mu^n \rangle} - Y_i]}{\sum_i A_{ij} \langle A_i, \mu^n \rangle d_i e^{-\langle A_i, \mu^n \rangle}}$$

Equation 6
Ziegler 2007

- Using an ordered subset method, Ziegler demonstrated that ML reconstruction can result in a signal to noise improvement of about 3 for equal resolution relative to filtered backprojection methods (FBP).

Ziegler, Medical Physics, 2007

Center midway edge

FPB =>

ITR => (OSC)

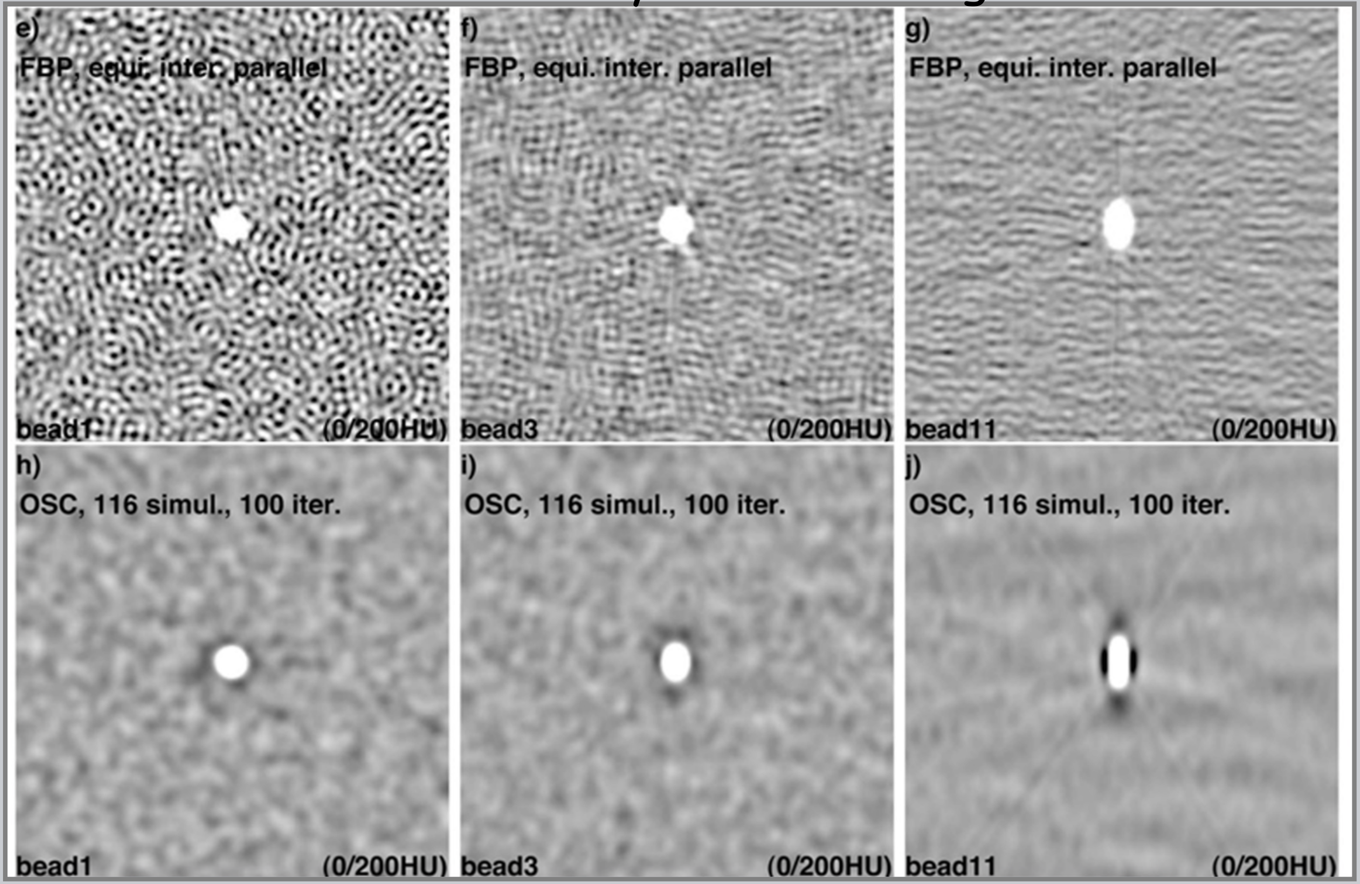

Ziegler, Medical Physics, 2007

Ziegler, Medical Physics, 2007

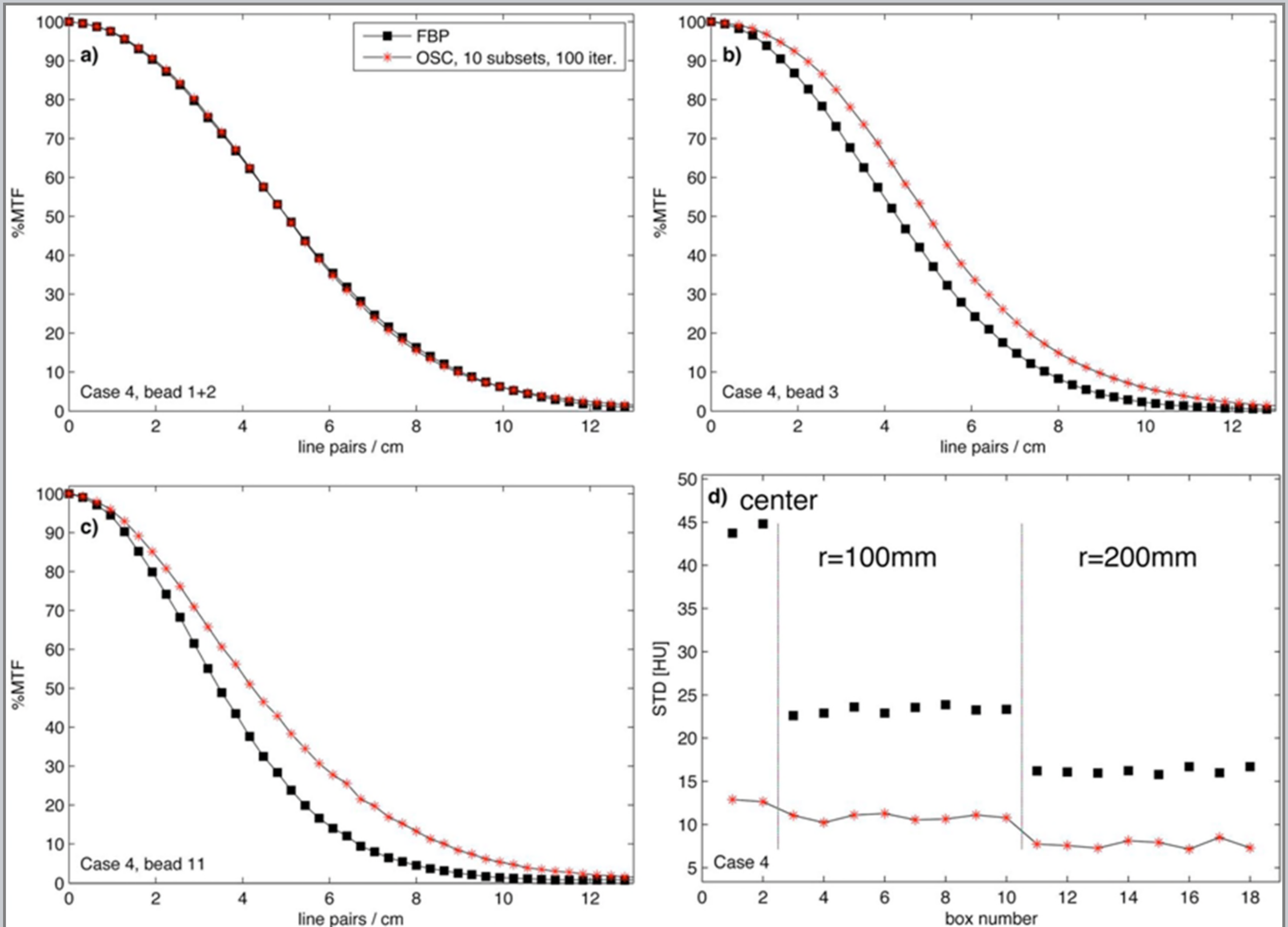

Hara 2009

Adaptive Statistical Iterative Reconstruction, GE Medical Systems.

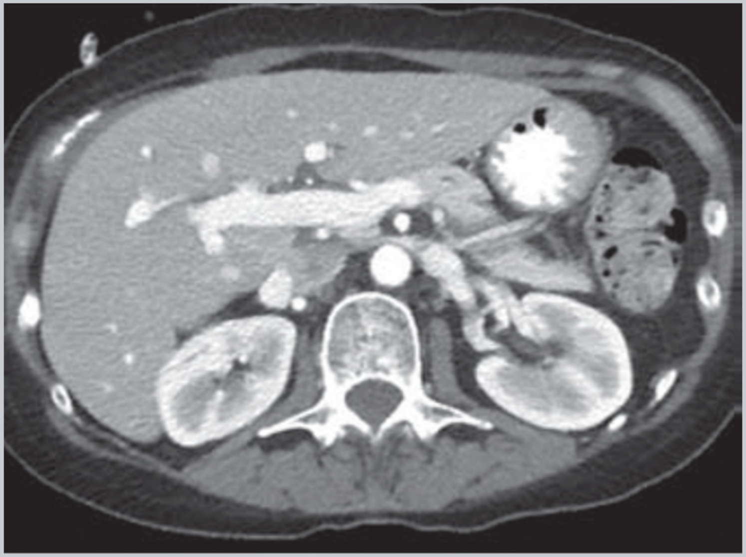

Dose Index = 8

ASIR

Dose Index = 22

Traditional Reconstruction

Geyer et. al., Iterative CT Reconstruction Techniques (review), Radiology, Aug. 2015

GE Medical Systems.

2008 – ASIR : Adaptive Statistical Iterative Reconstruction
2010 – VEO : Model based (computationally intensive)
2013 - ASIR-V : Hybrid ASIR-VEO

Philips Medical Systems.

2010 – iDose4 : Adaptive Statistical Iterative Reconstruction.
2013 – IMR : Model based reconstruction.

Siemens Medical Systems.

2008 – IRIS : Iterative reconstruction in image space.
2010 – SAFIRE : Sinogram affirmed iterative reconstruction
2015 – ADMIRE : Advanced modeled iterative reconstruction.

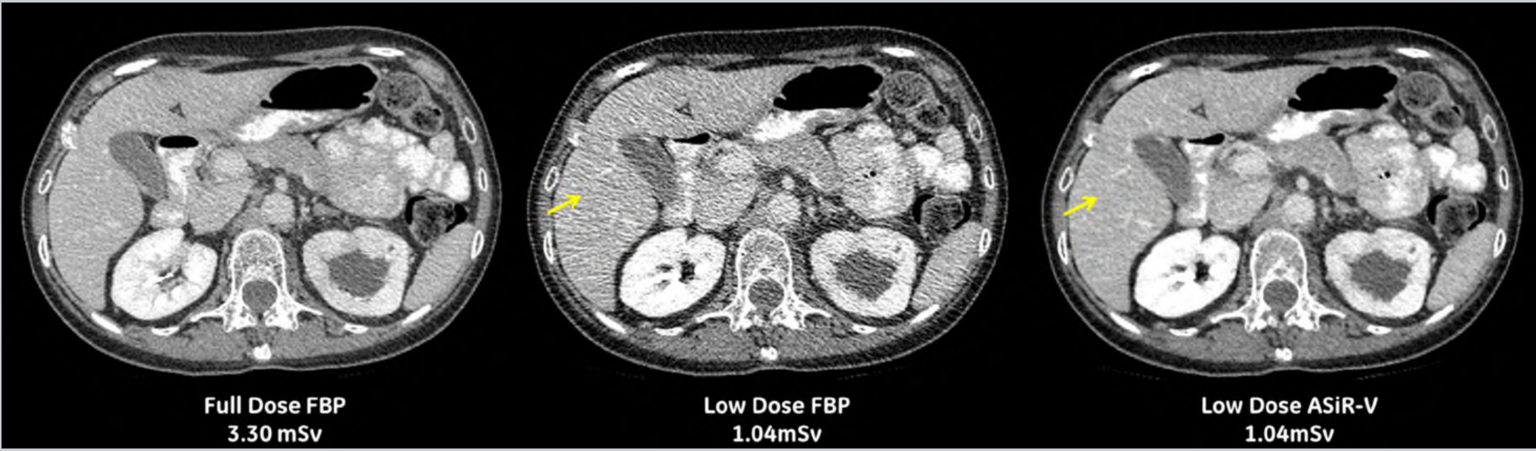

VII.B.5 – Model based IR

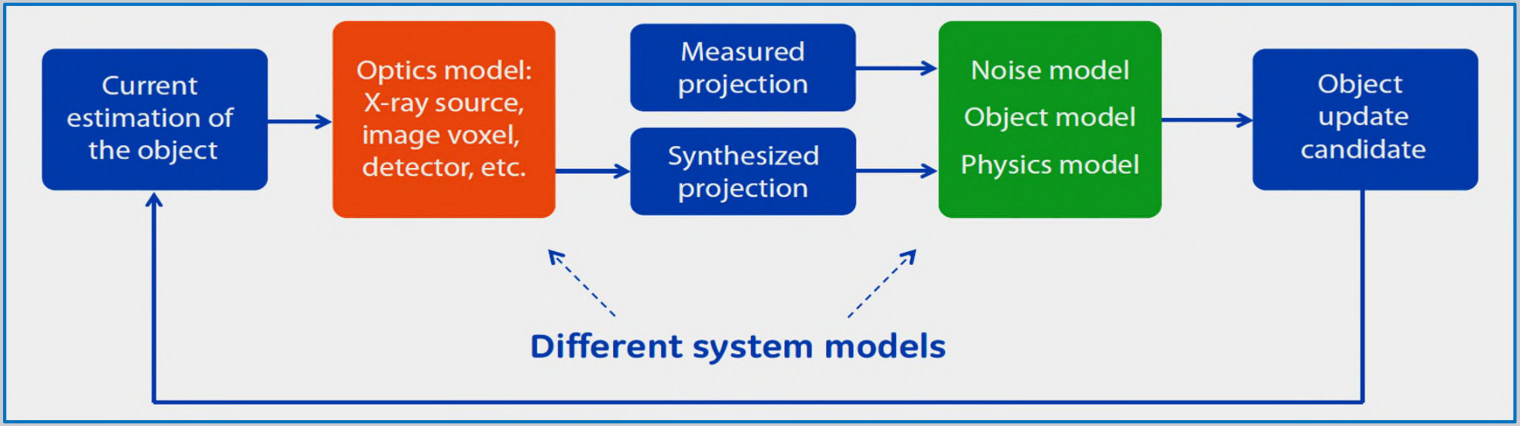

Model based IR:

- Rather than treating all measurements with equal weighting, a statistical model allows differing degrees of credibility among data.
- Three dimensional models describe the date acquisition process (source, gantry geometry, active detector) including the radiation interactions in a 3D model of the subject.
- Most IR methods specify a parameter that influences the amount of noise reduction.

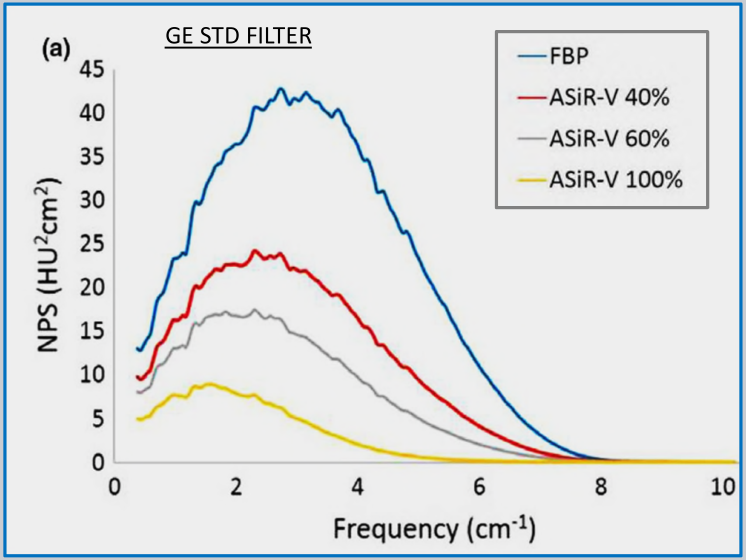

De Marco, J. Appl. Clin.. Med. Phys., Jan. 2018

VII.B.5 – ASIR-V vs ASIR

Kwon, Brit. J. Rad., Oct 2015

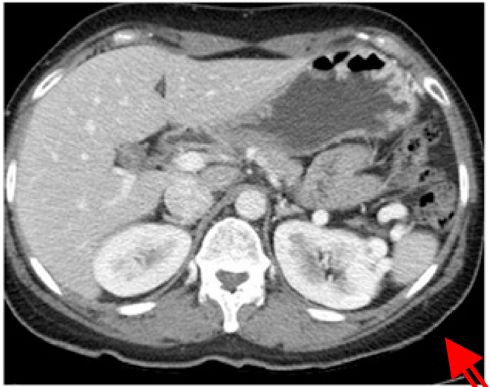

8.4 mGy ASIR 40%

4.7 mGy FBP

4.7 mGy ASIR 40%

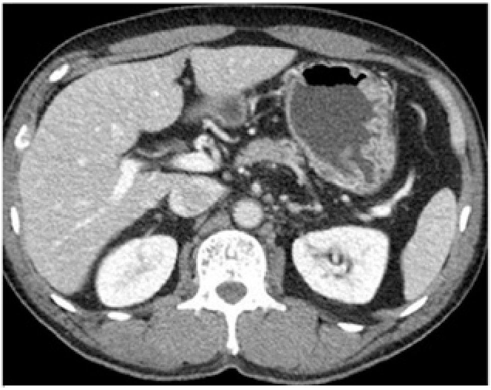

4.7 mGy ASIR-V 30%

4.7 mGy ASIR-V 50%

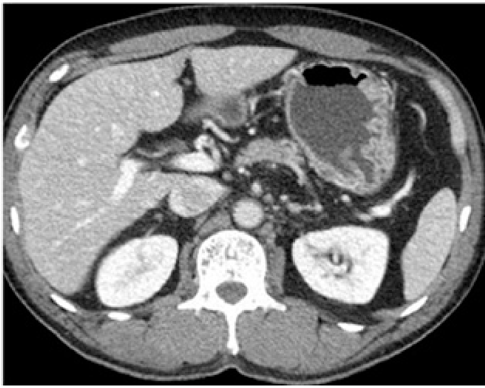

4.7 mGy ASIR-V 70%

The authors conclude that the 4.7 mGY ASIR-V 50% images are nearly identical in image noise, sharpness and diagnostic acceptability to the 8.4 mGy ASIR 40%

Kwon, Brit. J. Rad., Oct 2015

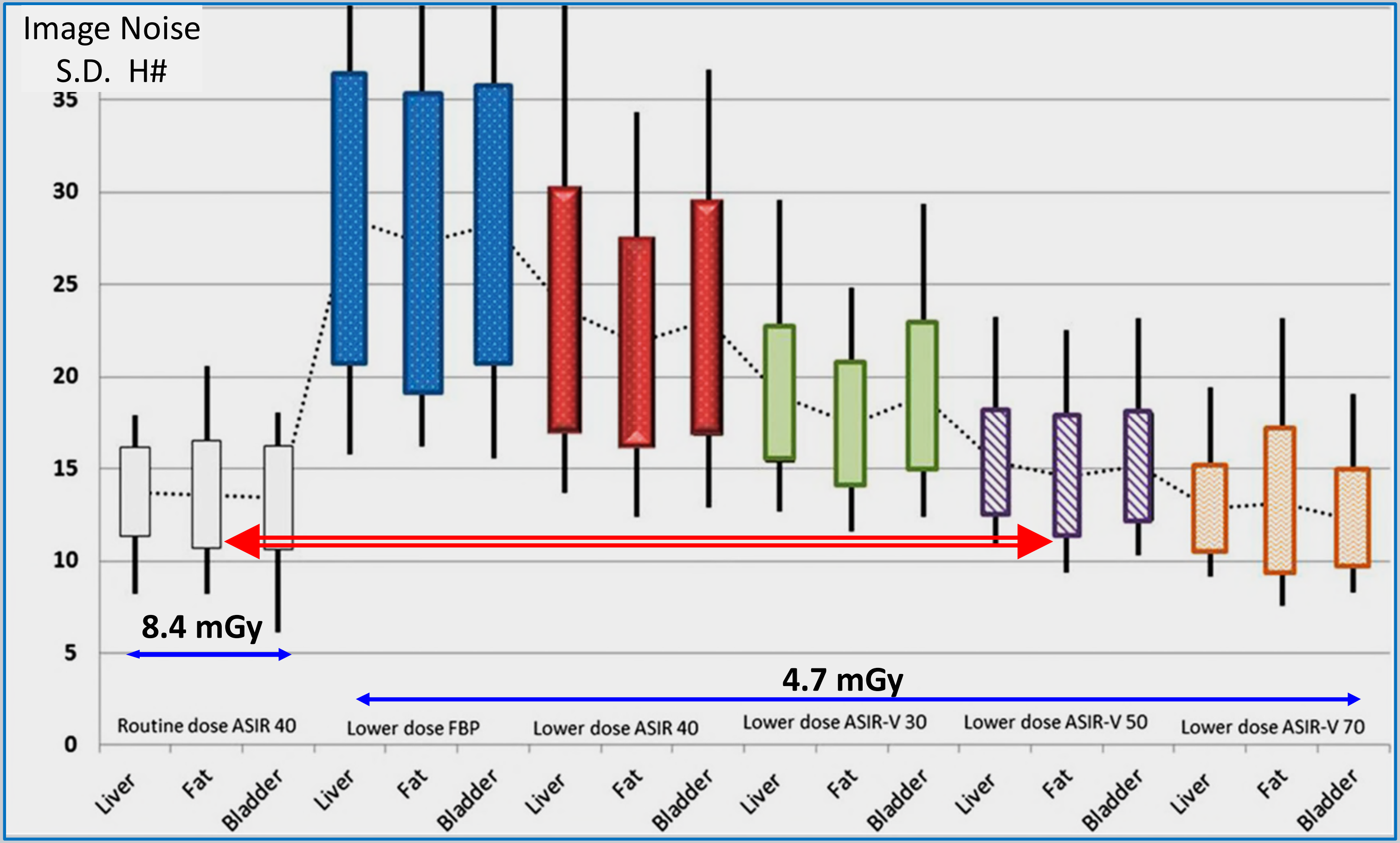

The authors conclude that the 4.7 mGY ASIR-V 50% images are nearly identical in image noise, sharpness and diagnostic acceptability to the 8.4 mGy ASIR 40%

?